Redox Biology 60 (2023) 102629

Contents lists available at ScienceDirect

Redox Biology

journal homepage: www.elsevier.com/locate/redox

Hydrogen sulfide as an anti-calcification stratagem in human aortic valve: Altered biogenesis and mitochondrial metabolism of H_2S lead to H_2S deficiency in calcific aortic valve disease

Zsolt Combi [a,b,c,1], László Potor [a,b,c,1], Péter Nagy [d,e,f], Katalin Éva Sikura [a,b,c], Tamás Ditrói [d], Eszter Petra Jurányi [d,g], Klaudia Galambos [c,d], Tamás Szerafin [h], Péter Gergely [i], Matthew Whiteman [j], Roberta Torregrossa [j], Yuchao Ding [a,c], Lívia Beke [k], Zoltán Hendrik [i], Gábor Méhes [k], György Balla [b,c,l], József Balla [a,b,c,*]

[a] Division of Nephrology, Department of Internal Medicine, Faculty of Medicine, University of Debrecen, Hungary
[b] ELKH-UD Vascular Pathophysiology Research Group, University of Debrecen, 11003, Hungary
[c] Kálmán Laki Doctoral School, University of Debrecen, Debrecen, Hungary
[d] Department of Molecular Immunology and Toxicology and the National Tumor Biology Laboratory, National Institute of Oncology, Budapest, Hungary
[e] Institute of Chemistry, Faculty of Science and Technology, University of Debrecen, Debrecen, Hungary
[f] Department of Anatomy and Histology, ELKH Laboratory of Redox Biology, University of Veterinary Medicine, Budapest, Hungary
[g] Doctoral School of Molecular Medicine, Semmelweis University, Budapest, Hungary
[h] Department of Cardiac Surgery, Faculty of Medicine, University of Debrecen, Hungary
[i] Institute of Forensic Medicine, Faculty of Medicine, University of Debrecen, Hungary
[j] University of Exeter Medical School, St. Luke's Campus, Magdalen Road, Exeter, EX1 2LU, UK
[k] Institute of Pathology, Faculty of Medicine, University of Debrecen, Hungary
[l] Department of Pediatrics, Faculty of Medicine, University of Debrecen, Hungary

ARTICLE INFO

Keywords:
Valvular inflammation
Arteriosclerosis
Chronic kidney disease
Phosphate
Vascular calcification
Hydrogen sulfide
Mitochondrial H_2S catabolism

ABSTRACT

Hydrogen sulfide (H_2S) was previously revealed to inhibit osteoblastic differentiation of valvular interstitial cells (VICs), a pathological feature in calcific aortic valve disease (CAVD). This study aimed to explore the metabolic control of H_2S levels in human aortic valves.

Lower levels of bioavailable H_2S and higher levels of interleukin-1β (IL-1β) and tumor necrosis factor-α (TNF-α) were detected in aortic valves of CAVD patients compared to healthy individuals, accompanied by higher expression of cystathionine γ-lyase (CSE) and same expression of cystathionine β-synthase (CBS). Increased biogenesis of H_2S by CSE was found in the aortic valves of CAVD patients which is supported by increased production of lanthionine. In accordance, healthy human aortic VICs mimic human pathology under calcifying conditions, as elevated CSE expression is associated with low levels of H_2S. The expression of mitochondrial enzymes involved in H_2S catabolism including sulfide quinone oxidoreductase (SQR), the key enzyme in mitochondrial H_2S oxidation, persulfide dioxygenase (ETHE1), sulfite oxidase (SO) and thiosulfate sulfurtransferase (TST) were up-regulated in calcific aortic valve tissues, and a similar expression pattern was observed in response to high phosphate levels in VICs. AP39, a mitochondria-targeting H_2S donor, rescued VICs from an osteoblastic phenotype switch and reduced the expression of IL-1β and TNF-α in VICs. Both pro-inflammatory cytokines aggravated calcification and osteoblastic differentiation of VICs derived from the calcific aortic valves. In contrast, IL-1β and TNF-α provided an early and transient inhibition of VICs calcification and osteoblastic differentiation in healthy cells and that effect was lost as H_2S levels decreased. The benefit was mediated via CSE induction and H_2S generation.

* Corresponding author. Department of Internal Medicine, Faculty of Medicine, University of Debrecen, 4012, Debrecen, Nagyerdei blvd. 98, Hungary.
E-mail addresses: balla.jozsef@med.unideb.hu, balla@belklinika.com (J. Balla).
[1] The authors share the first authorship.

https://doi.org/10.1016/j.redox.2023.102629
Received 16 January 2023; Accepted 6 February 2023
Available online 8 February 2023

We conclude that decreased levels of bioavailable H_2S in human calcific aortic valves result from an increased H_2S metabolism that facilitates the development of CAVD. CSE/H_2S represent a pathway that reverses the action of calcifying stimuli.

Abbreviations

ApoE$^{-/-}$	(apolipoprotein E knockout mice)
BCA	(bicinchoninic acid)
CAVs	(calcific aortic valves)
CAVD	(calcific aortic valve disease)
CAV-VICs	(calcified aortic valve-derived interstitial cells)
CBS	(cystathionine β-synthase)
CHAPS	(3-[(3-cholamidopropyl)dimethylammonio]-1-propanesulfonate)
CKD	(chronic kidney disease)
CSE	(cystathionine γ-lyase)
DMSO	(dimethyl sulfoxide)
ETHE1	(persulfide dioxygenase)
FA	(formic acid)
FBS	(fetal bovine serum)
GAPDH	(glyceraldehyde-3-phosphate dehydrogenase)
HAVs	(healthy aortic valves)
HAV-VICs	(healthy aortic valve-derived interstitial cells)
HEPES	(4-(2-hydroxyethyl)-1-piperazineethanesulfonic acid)
IL-1β	(interleukin-1β)
LC-MS/MS	(liquid chromatography tandem mass spectrometry)
MB	(methylene blue)
MPST	(mercaptopyruvate sulfurtransferase)
NNDP	(dimethyl-p-phenylenediamine dihydrochlorides)
PBS	(phosphate buffered saline)
RIPA	(radioimmunoprecipitation assay buffer)
SDS	(sodium dodecyl sulfate)
SO	(sulfite oxidase)
SQR	(sulfide quinone oxidoreductase)
STED	(Stimulated Emission Depletion)
TCA	(trichloroacetic acid)
TNF-α	(tumor necrosis factor-α)
TST	(thiosulfate sulfurtransferase)
VICs	(valvular interstitial cells)

1. Introduction

Calcific aortic valve disease (CAVD) is the most common valvular heart disease with high morbidity and mortality [1]. CAVD is an active disease, the affected valves are characterized by calcification and inflammation [1–5]. It was shown previously that pro-inflammatory cytokines, including interleukin-1β (IL-1β) and tumor necrosis factor α (TNF-α) are associated with CAVD, and inflammation is a hallmark of CAVD [1,5,6].

It has been revealed that valvular interstitial cells (VICs) trans-differentiate into osteoblast-like cells resulting in calcification of the aortic valve in CAVD [7,8]. The progression of CAVD is pronounced in patients with diabetes and chronic kidney disease (CKD) [9]. Hyper-phosphatemia is an independent cardiovascular risk factor in CKD [10, 11], and it has been linked to vascular calcification [9,12–14]. One of the most potent inducers of osteoblastic transdifferentiation and vascular calcification is elevated plasma phosphate levels [15–17].

It is well established that H_2S exhibits physiological functions by maintaining vascular homeostasis [18–23]. In animal models, it was revealed that a decrease in endogenous H_2S generation promotes atheroma formation in CSE-knockout mice, which is counteracted by exogenous sodium hydrosulfide (NaSH) treatment [24]. Furthermore, CSE expression was found to control flow-dependent vascular remodeling in disturbed flow regions of the vasculature [25]. In human studies, it has been found that patients with vascular diseases have significantly lower concentrations of circulating sulfide compared to healthy controls [26–28]. Moreover, patients with lower blood H_2S levels were shown to have lower post-operative survival after surgical revascularization [28].

Intracellular H_2S levels are tightly controlled by its biogenesis and efficient oxidative catabolism in the mitochondria [29]. H_2S can be generated via enzymatic routes including cystathionine γ-lyase (CSE) [30], cystathionine β-synthase (CBS) [31] and mercaptopyruvate sulfurtransferase (MPST) enzymes [32]. The canonical H_2S catabolizing oxidation pathway proceeds through a series of mitochondrial enzymes consisting of sulfide: quinone oxidoreductase (SQR) [33–35], persulfide dioxygenase (ETHE1) [36], thiosulfate sulfurtransferase (TST) [37] and sulfite oxidase (SO) [38,39].

Mitochondria-targeted H_2S donor, AP39 was developed as a useful pharmacological tool to study the mitochondrial physiology of H_2S in health and disease [40]. The rationale for targeted delivery of H_2S to the mitochondria is based on the evidence that H_2S can attenuate mitochondrial reactive oxygen generation and preserves mitochondrial integrity [41].

Previously, our laboratory demonstrated that endogenous H_2S generated by CSE controls mineralization and osteoblastic transition of human vascular smooth muscle cells [27] and human aortic VICs [42], and that CSE inhibits calcification of aortic valves in apolipoprotein E knockout mice (ApoE$^{-/-}$) [43]. It was also shown that the inhibitory effect of H_2S on aortic valve calcification is connected to its inflammation-controlling function [43]. Therefore, the objective of this current study was to investigate the control of H_2S levels in aortic valves of CAVD patients and to assess the calcification potential of human aortic valvular interstitial cells in the calcifying environment and their response to proinflammatory cytokines.

2. Materials and methods

2.1. Materials

All chemicals were analytical reagent grade or higher and were obtained from Sigma-Aldrich, (St Louis, MO, USA). The sulfide donor molecule used in our experiments - AP39 [(10-oxo-10-(4-(3-thioxo-3H-1,2-dithiol-5yl) phenoxy)decyl) triphenylphosphonium bromide] - was synthesized in our laboratory [44–46]. The sulfide stock solutions were freshly prepared in physiological saline before treatments. β-(4-hydroxyphenyl)ethyl iodoacetamide (HPE-IAM) was purchased from Santa Cruz Biotechnology (Dallas, TX, USA).

2.2. Human tissue samples and cell isolation

The cusps of human aortic valve leaflets were obtained from patients with severe calcified aortic valve disease who underwent valve replacement. The cusps of human aortic valve leaflets were obtained between August 2018 and May 2021 (58 patients) (Regional Research

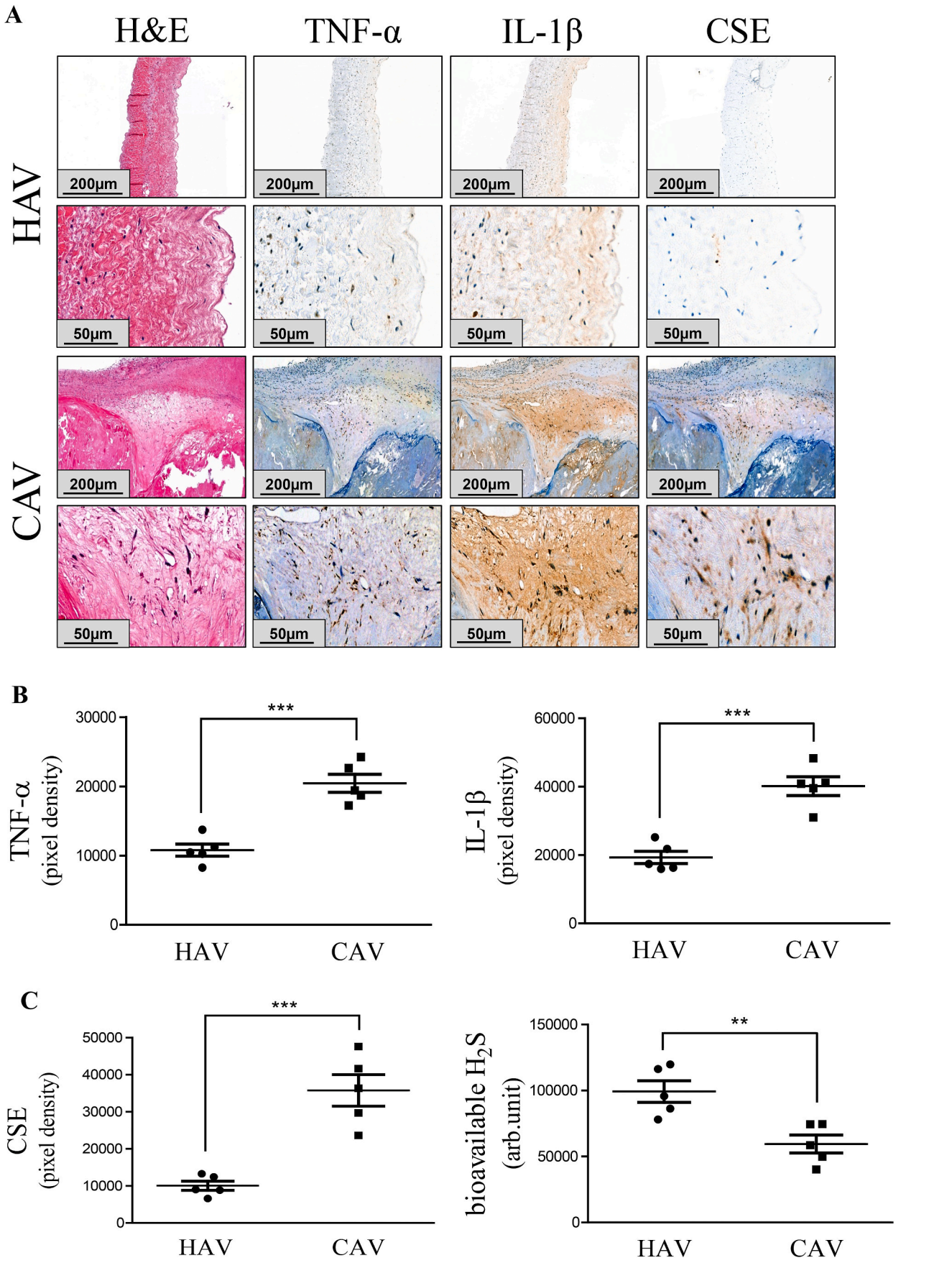

(caption on next page)

Fig. 1. Decreased levels of bioavailable hydrogen sulfide and high expression of inflammatory cytokines are characteristics of human calcific aortic valves
(A) Hematoxylin and eosin, TNF-α, IL-1β, and CSE immunohistochemical (IHC) stainings were performed on healthy aortic valves (HAVs) derived from the Department of Forensic Medicine, University of Debrecen (N = 5) and on calcific aortic valves (CAVs) of patients diagnosed with CAVD undergoing total aortic valve replacement (N = 5). Scale bars shown in the images represent 200 μm or 50 μm. (B) Quantitative analysis of TNF-α, and IL-1β IHC staining of tissue sections were calculated using ImageJ software (N = 5) (C, left panel). Quantitative analysis of CSE IHC staining of tissue sections was calculated using ImageJ software (N = 5) (C, right panel). Levels of bioavailable H_2S of healthy aortic valves and calcific aortic valves measured with LC-MS/MS are shown (N = 5). Results were analyzed by unpaired *t*-test and are shown as mean values ± SEM of five independent experiments. $^{**}p < 0.01$; $^{***}p < 0.001$.

Ethical Committee, Project No.: 61538-2/2017/EKU and 5643-2021). Healthy aortic valves (HAVs) were obtained from cadavers (N = 5) of suicide or traumatic events without cardiovascular diseases from the Department of Forensic Medicine, University of Debrecen (Regional Research Ethical Committee, Project No.: 5038-2018). VICs were isolated from human heart valves using collagenase type two (600 U/ml^{-1}) (Worthington Biochemical Corp.) and cultured as previously described [47]. All our experiments were performed on cells derived from 5 different donors in phenol red-free media.

2.3. Induction of inflammation in human healthy and calcified aortic valve derived VICs

Healthy aortic valve-derived interstitial cells (HAV-VICs) and calcified aortic valve-derived interstitial cells (CAV-VICs) were cultured in a calcification medium (2.5 mmol/L inorganic phosphate and 1.8 mmol/L calcium-chloride) with or without 10 nmol/L TNF-α or IL-1β, without phenol red for 5 days.

2.4. Induction of calcification, calcium measurement, Alizarin Red S staining

At approximately 80% confluence, VICs were cultured in a calcification medium with or without phenol red supplemented with 2.5 mmol/L inorganic phosphate and 1.8 mmol/L calcium chloride for 5 days. For time-dependent experiments, the first day of culturing in calcification medium was considered as day 0.

VICs were washed twice with phosphate-buffered saline (PBS) and decalcified using 0.6 mol/L hydrochloric acid (HCl). The calcium contents of the supernatants were assigned by QuantiChrome Calcium Assay Kit (Gentaur; 65-DICA-500), normalized to protein content.

Alizarin Red S (Sigma Aldrich; A5533) stainings were used to visualize calcium deposition. Cells were fixed with 3.7% formaldehyde for 10 min at 4 °C and stained with 2% Alizarin Red S. Stained cells were visualized using Leica DMIL LED microscope, Leica DMC4500 camera with Leica application suite LAS Software 4.9.0× and 10× magnification). Calcified regions were evaluated by ImageJ software.

2.5. Alkaline phosphatase staining

To visualize alkaline phosphatase activity, cells were cultured in 24 well plates and fixed in Citrate-acetone solution (2:3) followed by staining with Naphtanol AS-MX –Fast Violet B solution (Sigma; 1596-56-1). Cells were visualized using Leica DMIL LED microscope, Leica DMC4500 camera with Leica application suite LAS Software 4.9.0×, 10× magnification. Calcified areas were measured by ImageJ software.

2.6. Quantitative real-time PCR (qRT-PCR)

VICs were cultured in growth media and calcification media supplemented with 5 nmol/L AP39. After 5 days cells were harvested. Total RNA was isolated using RNAzol STAT-60 according to the manufacturer's instructions (TEL-TEST Inc., Friendswood, TX, USA). RNA concentrations were measured with a NanoDropTM 2000c spectrophotometer (Thermo Scientific Inc., Waltham, MA, USA). Subsequently, cDNA synthesis was performed using a high-capacity cDNA kit (Applied Biosystems, Foster City, CA). We used real-time PCR technique for quantification of mRNA levels of TNF-α (Thermo Fisher Scientific Inc.; HS00174128) and IL-1β (Thermo Fisher Scientific Inc.; HS0155410) and GAPDH (Thermo Fisher Scientific Inc.; HS02758991). TaqMan Universal PCR Master Mix was purchased from Applied Biosystems (Applied Biosystems, Foster City, CA). Finally, we performed TaqMan quantitative PCR (40 cycles at 95 °C for 15 s and 60 °C for 1 min) on 96-well plates with the Bio-Rad CFX96 (Bio-Rad Laboratories Inc., Hercules, California, USA) detection system. Results were expressed as mRNA expression normalized to GAPDH.

2.7. Western blot

The following primary antibodies were used in the project: rabbit anti-human TNF-α (Thermo Fisher Scientific; PA5-19810; 400 ng/mL), rabbit anti-human IL-1β (Invitrogen; 17 h18l16; 400 ng/mL), rabbit anti-human ALP (Abcam; ab65834; 1000 ng/mL), rabbit anti-human CSE (Proteintech Group; 12217-1-AP; 1000 ng/mL); rabbit anti-human SO (Thermo Fisher Scientific; PA5-21705; 1 mg/mL), rabbit anti-human ETHE1 Thermo Fisher Scientific; PA5-56040; 0,30 mg/mL), rabbit anti-human SQR (Proteintech Group; 17256-1-AP; 550 μg/mL), rabbit anti-human TST (Abcam; ab166625; 0.08 mg/mL) and rabbit anti-human CBS (Proteintech Group; 14787-1-AP; 700 μg/mL). HRP-labeled anti-rabbit or anti-mouse IgG secondary antibodies were used. Complexes of antigen-antibody were visualized with a horseradish peroxidase chemiluminescence detection system (Amersham Biosciences; RPN2109). After developing signals, membranes were stripped and incubated with glyceraldehyde-3-phosphate dehydrogenase (GAPDH).

2.8. Immunofluorescence staining

VICs were cultured on the coverslip and treated with and without calcification medium in the absence of phenol red, supplemented with 5 nmol/L AP39 for 5 days. After treatment, the cells were fixed with 3.7% formaldehyde for 15 min and blocked with 10% goat serum for 1 h at room temperature. Mouse anti-human TNF-α (Santa Cruz; sc-52746; 100 μg/mL) and rabbit anti-human IL-1β (Invitrogen; 17h18116; 400 ng/mL) at 1:500 dilution were used as primary antibodies to show levels of TNF-α and IL-1β in VICs. TNF-α antibody was labeled with goat anti-mouse Alexa Fluor 488 fluorophore (Thermo Fisher Scientific; A11004) and IL-1β was labeled with goat anti-rabbit Alexa Fluor 488 fluorophore (Thermo Fisher Scientific; A11070) for 1 h in dark at room temperature. All secondary antibodies were used at 1:500 dilution. Hydroxyapatite crystals were stained with IVI Sense Osteo 680 Fluorescent Probe (OsteoSense; PerkinElmer®; NEV10020EX). Hoechst 33258 was used to stain nuclei. Multicolor STED imaging was acquired with STED (Stimulated Emission Depletion) Leica TCS SP8 gated STED-CW nanoscopy (Leica Microsystem Mannheim, Germany). Gated STED images were deconvolved using Huygens Professional (Scientific Volume Imaging B. V., Hilversum, Netherlands) software. Levels of TNF-α and IL-1β were evaluated by Image J software. Separate images of immunofluorescence stainings (nucleus, osteosense, IL-1β, and TNF-α) with their antibody controls can be found in the Supplementary Fig. 3.

2.9. Determination of sulfide levels from cell lysates with modified methylene blue assay

Sulfide levels were measured with zinc precipitation method according to Gilboa-Garber et al. [48] and A. D. Ang et al. [49]. Cell lysates (50 μL) were mixed with 350 μL 1% zinc acetate and 50 μL 1.5 mol/L

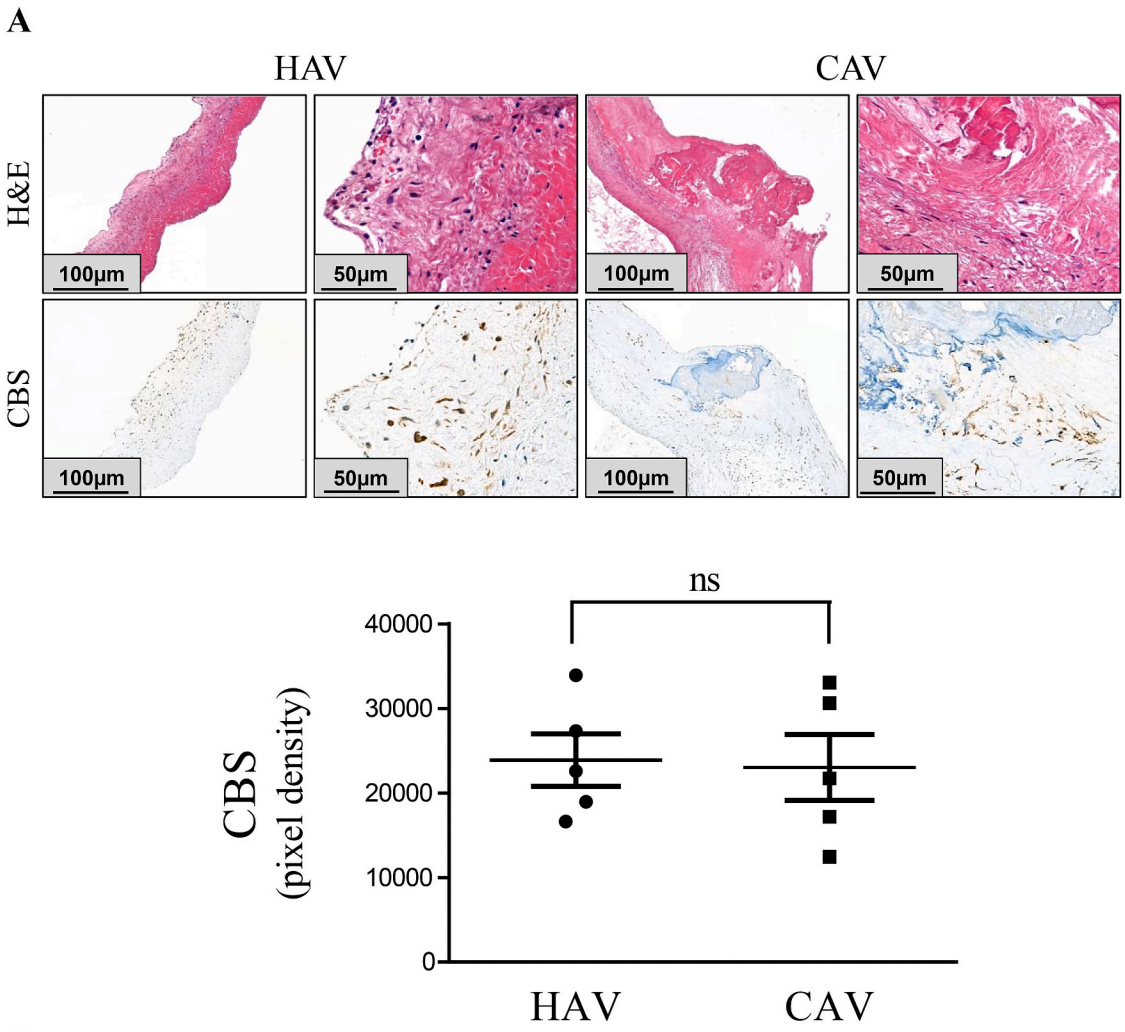

(caption on next page)

Fig. 2. Expression of cystathionine beta-synthase doesn't change in cavd
(A) Hematoxylin and eosin and CBS immunohistochemical (IHC) stainings were performed on healthy aortic valves (HAVs) derived from the Department of Forensic Medicine, University of Debrecen (N = 5) and on calcific aortic valves (CAVs) of patients diagnosed with CAVD undergoing total aortic valve replacement (N = 5). Scale bars shown in the images represent 100 μm or 50 μm. (B) HAVs (N = 4) and CAVs (N = 5) were cryogenically pulverized and taken up with cell lysis buffer followed by 5-s sonication on ice three times. CBS protein expression normalized to GAPDH of healthy human aortic valves (N = 4) and calcified human aortic valves (N = 5) were measured with western blot. Quantitative analysis of the CBS western blot was calculated using ImageJ software. Results were analyzed by unpaired *t*-test and were shown as mean values ± SEM. Ns: not significant; *p < 0.05; ***p < 0.001.

sodium hydroxide and incubated for 60 min on a shaker. The incubation step was followed by centrifugation at 2000*g* for 5 min to pellet the generated zinc sulfide. The supernatant was then removed, and the pellet was washed with 1 mL of distilled water by vortexing extensively, followed by centrifugation at 2000*g* for 5 min. The supernatant was then discarded and the pellet was reconstituted with 160 μL of distilled water and mixed with 40 μL of pre-mixed dye (20 μL of 20 mmol/L dimethyl-p-phenylenediamine dihydrochlorides (NNDP) in 7.2 mol/L HCl and 20 μL of 30 mmol/L iron (III) chloride ($FeCl_3$) in 1.2 mol/L HCl). After 10 min, the absorbance of the generated methylene blue (MB) was measured with a spectrophotometer at 667 nm. The concentrations were determined by the MB's extinction coefficient (30 200 $M^{-1}cm^{-1}$). Samples were normalized to protein content. Results are shown as μmol/L total H_2S/mg protein.

2.10. Dual silencing of cystathionine γ-lyase and cystathionine β-synthase

Transient silencing of cystathionine γ-lyase (CSE) and cystathionine β-synthase (CBS) genes using siRNAs (CSE: Ambion; 4392420; s3710; CBS: Ambion; 4390824; s289) were performed. Briefly, VICs were cultured in an antibiotic-free medium (D-MEM, Sigma) in 12 well plates. At approximately 70% confluence, cells were transfected with CSE and CBS siRNA for 4 h in minimal serum media (Opti-MEM, Gibco). After 4 h, 30% fetal bovine serum (FBS) containing, antibiotic-free D-MEM was added. The next day, cells were washed and treated with 2.5 mmol/L inorganic phosphate and 1.8 mmol/L calcium chloride further 10 nmol/L TNF-α or 10 nmol/L IL-1β cytokines every other day until 5 days.

2.11. Immunohistochemistry (IHC)

Heart valve tissues were fixed with 10% (v/v) neutral buffered formalin (NBF) for one day. After fixation, samples were dehydrated with ethanol and embedded in paraffin wax. IHC assays were performed on a VENTANA BenchMark Ultra automated staining instrument (Ventana Medical Systems), using VENTANA reagents except as noted, according to the manufacturer's instructions. Slides were deparaffinized using EZ Prep solution (Ventana medical systems; product number: 5279771001) for 4 min at 72 °C. For epitope retrieval, ULTRA Cell Conditioning 1 Solution (ULTRA CC1) was used (contains: Tris-based buffer and a preservative (Ventana medical systems; product no: 5424569001) at 100 °C, for 52 min. Antibodies used for IHC: rabbit anti-human TNF-α (Thermo Fisher Scientific; PA5-19810; 400 ng/mL); rabbit anti-human IL-1β (Invitrogen; 17 h18l16; 400 ng/mL); rabbit anti-human CSE (Proteintech Group; 12217-1-AP; 1000 ng/mL); and rabbit anti-human CBS (Proteintech Group; 14787-1-AP; 700 μg/mL. For detection, slides were developed using VENTANA ultraView Universal DAB detection kit (Ventana medical systems; product no: 5269806001) according to the manufacturer's instructions. Slides were then counterstained with hematoxylin II (Ventana medical systems; product no: 5277965001) for 12 min, followed by Bluing reagent (Ventana medical systems; product no: 5266769001) for 8 min. The intensity and distribution of antibody expression were assessed by light microscopy (Leica DM2500 microscope, DFC 420 camera, and Leica Application Suite V3 software, Wetzlar, Germany).

2.12. LC-MS/MS measurement of CSSC, cystathionine, lanthionine and HCys

Cryogenically pulverized tissues (N = 5) were resuspended in CHAPS buffer (150 mmol/L KCl, 50 mmol/L HEPES pH 7.4, 0.1% CHAPS, protease inhibitors) and sonicated for 10 s. After centrifugation (14 000 g 10 min, 4 °C) protein concentrations were measured from the supernatant using the BCA method. 50 μl of the samples at 1 mg/mL protein concentration was derivatized with the EZ:Faast kit (Phenomenex, Torrance, CA, USA) following the manufacturer's instructions and measured with a Thermo Vanquish UHPLC system coupled to a Thermo Q Exactive Focus mass spectrometer. m/z values for CSSC, Cystathionine and HCys recommended by the EZ:Faast kit were used, Lanthionine was monitored using published *m/z* values [50].

2.13. LC-MS/MS measurement of bioavailable H_2S

Measurement is based on the method published by Akaike et al. [51] as described here: cryogenically pulverized heart tissue was resuspended in ice-cold methanol containing 5 mmol/L β-(4-hydroxyphenyl)ethyl iodoacetamide (HPE-IAM). Between each preparation step, samples were kept on ice. After sonication the derivatizations were carried out at 37 °C for 20 min followed by centrifugation at 14 000 g for 10 min at 4 °C. 100 μL of the supernatants were acidified with 5 μL of 10% formic acid and diluted two-fold with 0.1% FA/H_2O before injection. Tissue pellets were dissolved in 1% SDS/PBS, sonicated and protein contents were measured using BCA assay. Liquid chromatography-tandem mass spectrometry (LC-MS/MS) measurements were carried out on a Thermo Q-Exactive Focus Orbitrap mass spectrometer coupled to a Thermo Vanquish UHPLC (ultra-high-performance liquid chromatograph). The derivatized analytes were separated on a Phenomenex Kinetex C18 (50 × 2.1 mm, 2.6 μm) column with eluents 0.1% FA/H_2O (A) and 0.1% FA/MeOH (B). The initial 5% B was linearly increased to 95% in 15 min, then lowered back to 5% B in 2 min and held there for 3 min before the next injection. Flow rate was 0.3 mL/min at 30 °C. MS/MS detection for the alkylated sulfide product was carried out in positive ionization mode, higher-energy collisional dissociation (HCD) was used to detect the 252 m/z fragment from the 389 m/z precursor ion.

2.14. LC-MS/MS measurement of protein persulfidation

Measurement is based on the method published by Akaike et al. [51] and performed as described here: Cryogenically pulverized heart tissues were resuspended in RIPA buffer containing 5 mmol/L HPE-IAM and sonicated. After centrifugation at 14 000 g for 10 min at RT, 100 μL of the supernatants were desalted using Zeba spin columns (7K MWCO, 0.5 mL). The protein contents of the flow-through were measured using BCA method, then 4 μL of 100 mmol/L HPE-IAM in DMSO was added. Protein levels of the desalted samples were brought to equal using RIPA buffer and digested with pronase (3 mg/mL) in 35 mmol/L Na-acetate buffer (pH 5.0) at 37 °C for 1 h. The samples were acidified with 10% TCA and centrifuged for 10 min at 14 000 g RT. The supernatants were injected onto the LC-MS/MS and the derivatized analytes were measured by using the LC-MS/MS method mentioned above under "LC-MS/MS measurement of bioavailable H_2S". MS/MS detection for cysteine and cysteine-persulfide was carried out in positive ionization mode, higher-energy collisional dissociation (HCD) was used to detect the 121 m/z fragment from 299 m/z (cysteine) and 331 m/z

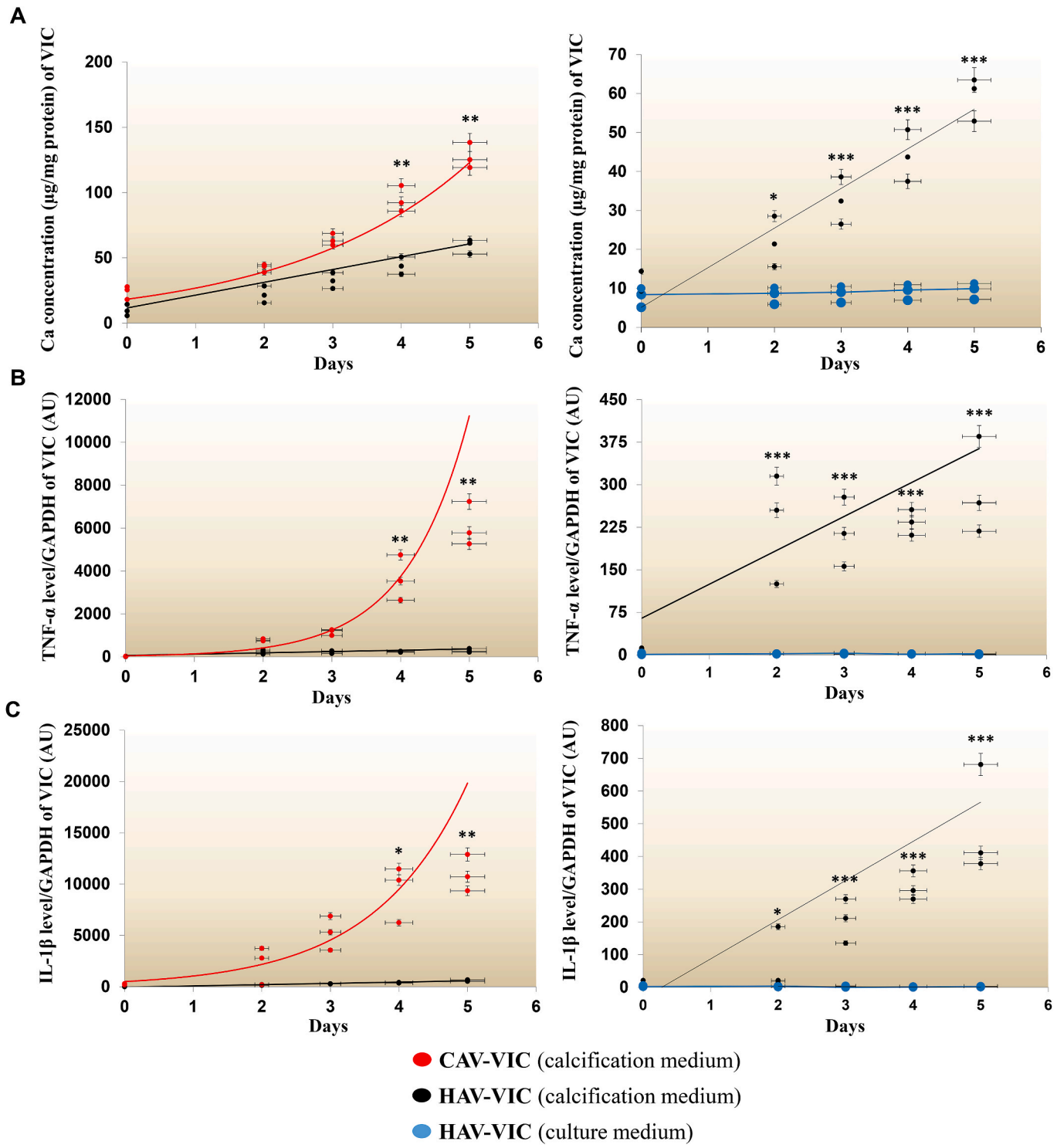

Fig. 3. Mineralization potential and inflammatory response of valvular interstitial cells to high levels of phosphate
Valvular interstitial cells (VICs) isolated from calcific aortic valves (CAV-VICs) or healthy aortic valves (HAV-VICs) were exposed to calcification medium supplemented with 2.5 mmol/L inorganic phosphate and 1.8 mmol/L calcium chloride every other day for 5 days. (A) Calcium contents of extracellular matrix normalized to a protein of VICs are shown (n = 3). (B) TNF-α levels normalized to GAPDH of VICs cultured in calcification medium or culture medium are shown (n = 3). (C) IL-1β levels normalized to GAPDH of VICs cultured in calcification medium or culture medium are shown (n = 3). Red lines indicate CAV-VICs cultured in calcification medium. Black lines indicate HAV-VICs cultured in calcification medium. Blue lines show the HAV-VICs maintained in culture medium. Results were analyzed by unpaired *t*-test and are shown as mean values ± SEM of three independent experiments. *$p < 0.05$; **$p < 0.01$. (For interpretation of the references to color in this figure legend, the reader is referred to the Web version of this article.)

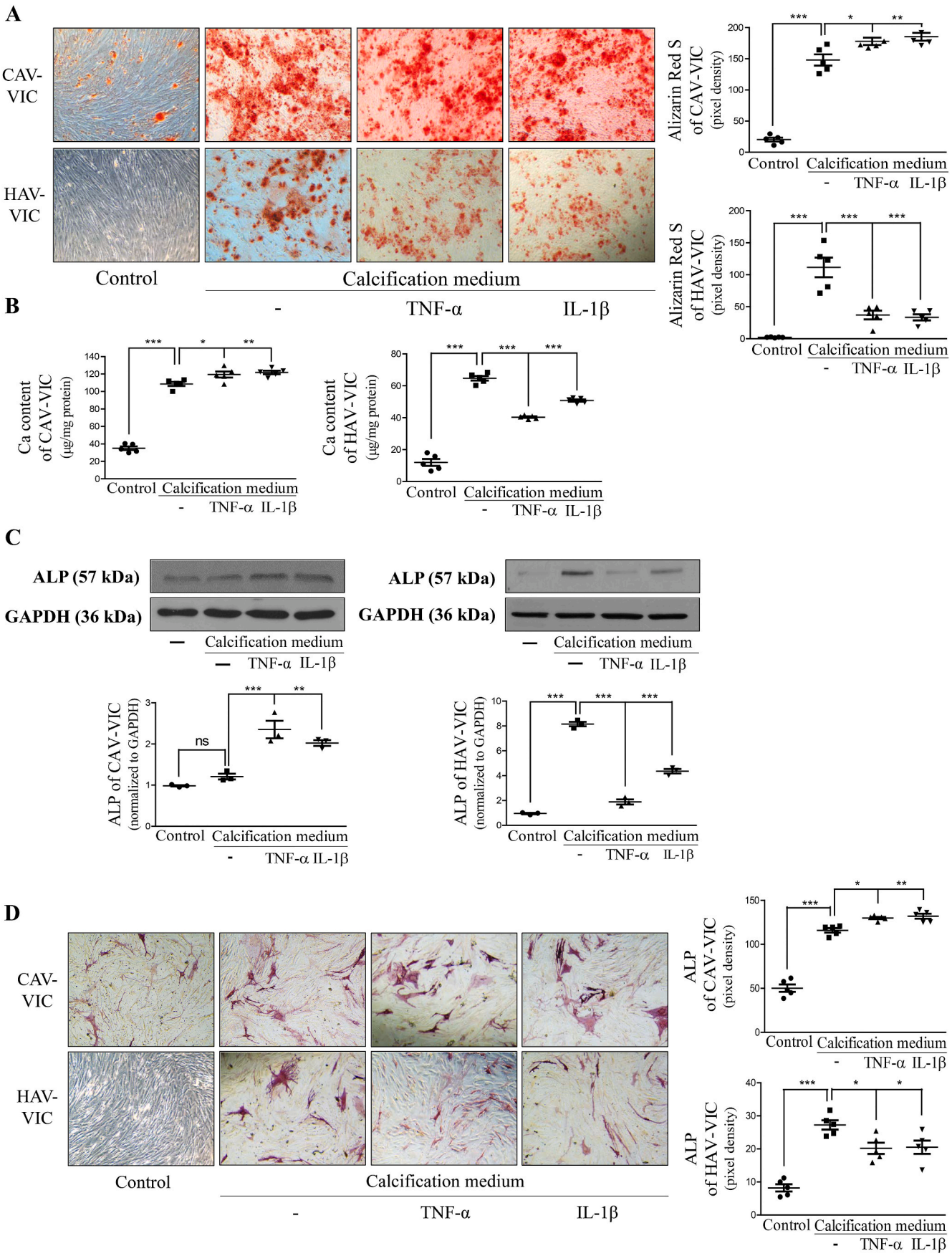

(caption on next page)

Fig. 4. Distinct calcification response of valvular interstitial cells to pro-inflammatory cytokines depending upon disease state
Valvular interstitial cells (VICs) isolated from calcific aortic valves (CAV-VICs) or healthy aortic valves (HAV-VICs) were cultured in growth medium or calcification medium, containing 2.5 mmol/L inorganic phosphate and 1.8 mmol/L calcium chloride every other day, for 5 days. VICs maintained in calcification media were exposed to TNF-α (10 nmol/L) or IL-1β (10 nmol/L) for 5 days. (A) Alizarin Red S staining of CAV-VICs (upper panels) and HAV-VICs (lower panels) are shown. Quantitative analysis of Alizarin Red S staining of CAV-VICs and HAV-VICs was calculated using ImageJ software (n = 5). (B) Extracellular calcium contents normalized to protein of CAV-VICs and HAV-VICs are shown (n = 5). (C) ALP protein expressions normalized to GAPDH of CAV-VICs (left panels) and HAV-VICs (right panels) were measured with western blot (n = 3). Quantitative analysis of the ALP western blots were calculated using ImageJ software. (D) ALP staining of CAV-VICs (upper panels) and HAV-VICs (lower panels) are shown. Quantitative analysis of ALP staining of CAV-VICs and HAV-VICs was calculated using ImageJ software (n = 5). Results were analyzed by one-way ANOVA, Bonferroni's Multiple Comparison Test, and are shown as mean values ± SEM of three (D and E) or five (A–C) independent experiments. IL-1β and TNF-α treatment were compared to the minus condition (calcification medium). Ns: not significant; *$p < 0.05$; **$p < 0.01$; ***$p < 0.001$. (For interpretation of the references to color in this figure legend, the reader is referred to the Web version of this article.)

(cysteine-persulfide) precursor ions.

2.15. Experimental units

"N" represents the number of tissue samples used in each group. The "n" denotes the number of replications of the independent results.

2.16. Statistical analysis

Data were analyzed by GraphPad Prism 5.02 software (GraphPad Software Inc., 7825 Fay Avenue, Suite 230 La Jolla, CA 92037). All statistical data are presented with mean ± SEM. If data groups passed the normality and equal variance tests, we performed Student's t-test or one-way ANOVA followed by Bonferroni post hoc tests as indicated in figure legends. $p < 0.05$ was considered significant.

3. Results

3.1. High expression of CSE and low bioavailable H_2S levels are accompanied by high expression of pro-inflammatory cytokines in CAVD

Since CAVD was revealed to be an inflammatory disease [1,5] and H_2S was found to control vascular calcification, we examined the expression of proinflammatory cytokines and CSE in human aortic valves. Valves from patients diagnosed with CAVD who underwent aortic valve replacement, were stained for cytokines IL-1β and TNF-α as well as for CSE. For controls, healthy aortic valves (HAVs) from cadavers of suicide or traumatic events without cardiovascular diseases were obtained. As shown in Fig. 1A and B, severe valvular calcification was accompanied by increased expression of IL-1β and TNF-α in calcific aortic valves (CAVs). Importantly, a significant enhancement of CSE expression was also detected in the aortic valves of patients diagnosed with CAVD as compared to HAVs (Fig. 1A and C/left panel). Since elevated CSE levels were found in the aortic valves of CAVD patients, we measured bioavailable H_2S levels in valvular tissues derived from CAVD patients and from healthy individuals employing LC-MS/MS. Surprisingly, aortic valvular tissues of CAVD patients had lower bioavailable H_2S levels compared to HAV tissues (Fig. 1C, right panel).

Besides CSE, cystathionine beta-synthase (CBS) is another enzyme that catalyzes the biosynthesis of hydrogen sulfide. For this reason, we examined the expression of CBS in healthy and calcified human aortic valves. Immunohistochemistry and western blot analyses demonstrated that CBS level was not changed in CAVs compared to the HAVs (Fig. 2A and B).

3.2. Mineralization and inflammatory response of VICs to high phosphate concentrations

To assess the mineralization potential and inflammatory response of VICs to calcifying stimuli, we exposed cells isolated from CAVs or HAVs to high phosphate concentrations, which are known to trigger the transition of cells towards an osteoblast phenotype [15]. As demonstrated in Fig. 3 (left panels), a robust response was detected in VICs derived from CAVD patients, which was reflected by the accumulation of calcium in the extracellular matrix and high levels of pro-inflammatory cytokines, IL-1β and TNF-α (red lines). VICs from healthy patients exhibited significantly less calcium deposition and lower expression of IL-1β and TNF-α with a significant delay (black lines) compared to cells from CAVD patients (red lines). We also assessed the cellular responses in VICs derived from healthy patients (Fig. 3, right panels) cultured in calcifying media (black lines) compared to cells maintained in normal culture media (blue lines). Please note the values on y-axis in right panels are significantly lower compared to those in left panels. As shown in the right panels (Fig. 3), calcification occurred and the levels of IL-1β and TNF-α were increased in VICs of HAVs as a result of phosphate exposure.

3.3. Pro-inflammatory cytokines increase calcification of human VICs derived from CAVD patients

As pro-inflammatory cytokines were previously revealed to play a central role in the initiation and progression of CAVD [1,3,5], we tested whether IL-1β and TNF-α enhance calcification of VICs provoked by high phosphate. As shown in Fig. 4A (upper panels) and B (left panel), phosphate treatment of VICs derived from CAVD patients resulted in the deposition of calcium in the extracellular matrix. Upon exposure to IL-1β or TNF-α, we found an increased accumulation of calcium in these cells compared to cells exposed to phosphate alone (Fig. 4A (upper panel) and B (left panel)). Accordingly, IL-1β or TNF-α treatment of VICs from CAVD patients maintained in high phosphate-containing media further increased the expression of alkaline phosphatase as demonstrated by westen blot analysis (Fig. 4C), and such induction was confirmed by ALP staining (Fig. 4D, upper panels). These data are consistent with the notion that transdifferentiation of valvular interstitial cells to an osteoblastic phenotype is connected to inflammation.

3.4. Transient inhibition of calcification is provoked by pro-inflammatory cytokines in human VICs derived from healthy aortic valves

To our surprise, as we exposed VICs derived from HAVs to IL-1β or TNF-α an inhibition of phosphate-induced calcification occurred. As shown in Fig. 4A (lower panels) and B (right panel), calcium accumulation developed within the extracellular matrix of VICs from healthy aortic valves maintained in high phosphate-containing media (second panel). Importantly, as demonstrated in Fig. 4A (lower third and fourth panels) and B (right panel), deposition of calcium was decreased as cells were exposed to IL-1β or TNF-α within a time period of 5 days, and such benefit was lost at day 14 (Fig. 5A). In accordance, both proinflammatory cytokines inhibited the expression of the osteoblast-specific gene, ALP as demonstrated by western blot analysis and ALP stainings (Fig. 4C/right panel and D/lower panels). These data indicate that IL-1β and TNF-α exhibit a transient inhibition on phosphate-induced osteoblastic phenotype switch in healthy aortic valve-derived VICs.

3.5. CSE/H_2S mediates the IL-1β and TNF-α evoked transient inhibition of human VICs calcification

To reveal the molecular mechanisms of the transient inhibition of the

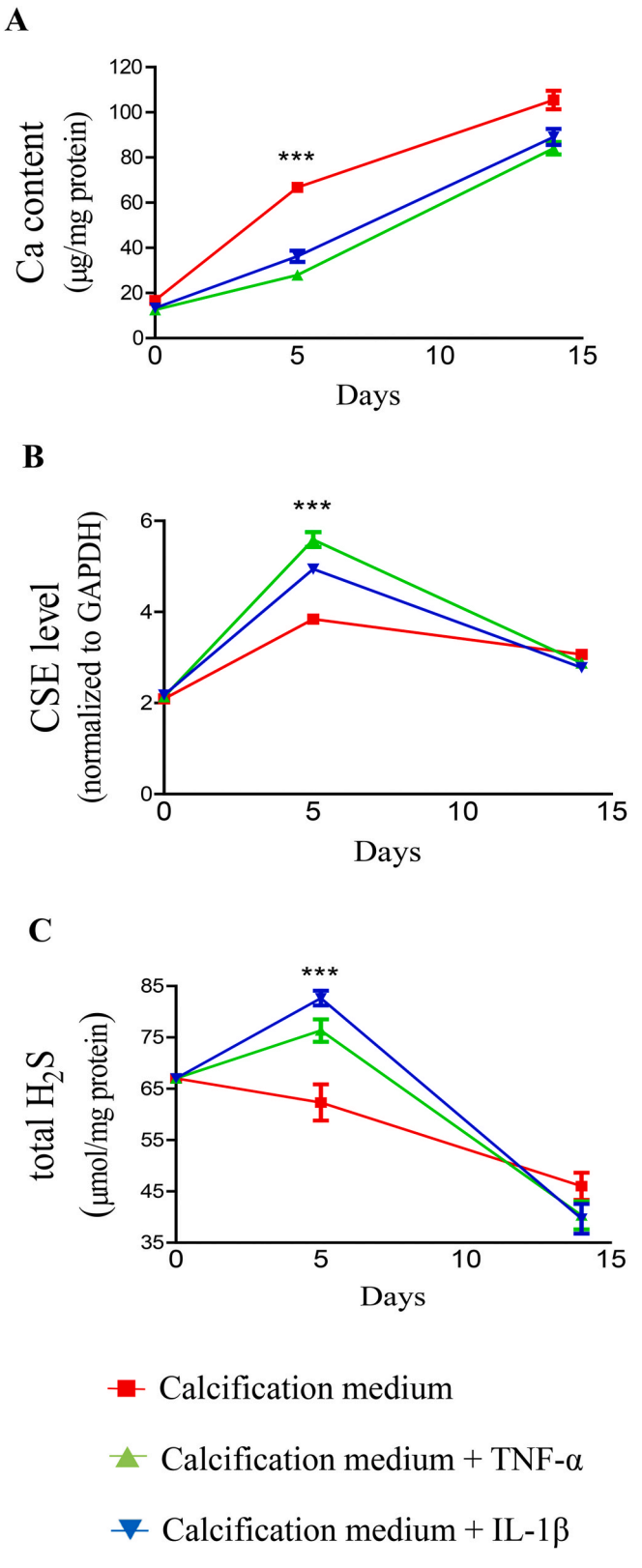

(caption on next column)

Fig. 5. Transient inhibition of valvular interstitial cell calcification provoked by pro-inflammatory cytokines is associated with elevated cystathionine-γ-lyase expression and H_2S generation.
Valvular interstitial cells isolated from healthy aortic valves (HAV-VICs) were cultured in calcification medium, containing 2.5 mmol/L inorganic phosphate and 1.8 mmol/L calcium chloride every other day, for 5 and 14 days. VICs maintained in calcification media were exposed to TNF-α (10 nmol/L) or IL-1β (10 nmol/L) for 5 and 14 days. (A) Calcium contents of extracellular matrix normalized to protein of HAV-VICs are shown (n = 3). (B) CSE protein expression normalized to GAPDH in HAV-VICs maintained in calcification media with or without TNF-α (10 nmol/L) and IL-1β (10 nmol/L) for 5 and 14 days are shown (n = 3). (C) H_2S generation measured with modified methylene blue method and normalized to protein of HAV-VICs are shown (n = 3). Results were analyzed by one-way ANOVA, Bonferroni's Multiple Comparison Test, and are shown as mean values ± SEM of three independent experiments. Ns: not significant; $*p < 0.05$; $**p < 0.01$; $***p < 0.001$. (For interpretation of the references to color in this figure legend, the reader is referred to the Web version of this article.)

phosphate-induced calcification in HAV-VICs provoked by proinflammatory cytokines we investigated the cellular H_2S pool in HAVs using the modified methylene blue method. A gradual decrease in total H_2S levels was found in VICs of healthy aortic valves maintained in high phosphate media (Fig. 5C). In contrast, in cells exposed to IL-1β or TNF-α, H_2S levels were elevated at 5 days followed by a decline at 14 days (Fig. 5C). We previously identified several triggers including IL-1β or TNF-α for inducing CSE expression in vascular cells [52]. Therefore, we measured the expression of CSE in HAV-VICs. Both IL-1β and TNF-α enhanced CSE protein levels in HAV-VICs (Fig. 5B) suggesting a CSE-mediated control of mineralization via endogenous H_2S production.

We previously observed that mitigation of endogenous H_2S production by lowering CSE and CBS expression promotes calcification of valvular interstitial cells [42]. Therefore, we tested whether the transient benefit of pro-inflammatory cytokines depends upon CSE levels. We found that both IL-1β and TNF-α lost their anti-calcification effects under calcifying conditions when interfering RNAs for CSE/CBS were used for 5 days as reflected by a significant increase in calcium deposition within the extracellular matrix of human VICs derived from HAVs (Fig. 6A).

We wondered if VICs isolated from the aortic valves of CAVD patients have elevated CSE levels in response to pro-inflammatory cytokines. As shown in Fig. 6B, while phosphate alone significantly enhanced CSE levels, neither IL-1β nor TNF-α altered the expression of CSE in VICs derived from CAVD patients' valves maintained in high phosphate-containing media. In contrast, in these cells cultured in high phosphate-containing media total H_2S levels measured with modified methylene blue method were lower compared to cells maintained in normal culture media (Fig. 6C). Moreover, treatment with IL-1β or TNF-α in calcification medium further decreased H_2S levels of cells derived from CAVD patients (Fig. 6C).

3.6. Increased mitochondrial metabolism of H_2S in aortic valves of CAVD patients

The increased expression of CSE in aortic valves of CAVD patients compared to healthy controls was found to be accompanied by diminished H_2S levels (Fig. 1C). This contra intuitive observation might suggest that the activity of CSE is reduced in CAVD tissues leading to decreased H_2S production. Therefore, to gain deeper insights into enzyme activities of the transsulfuration pathway we conducted sulfur metabolome analyses. Both cysteine and homocysteine levels were similar, but cystathionine levels were lower in the aortic valves of CAVD patients compared to healthy aortic valves (Fig. 7). These analytes are not only substrates but in different enzymatic routes they can also be products of CSE and other transsulfuration enzymes, so they are generated and consumed in interlinked enzymatic pathways. A more

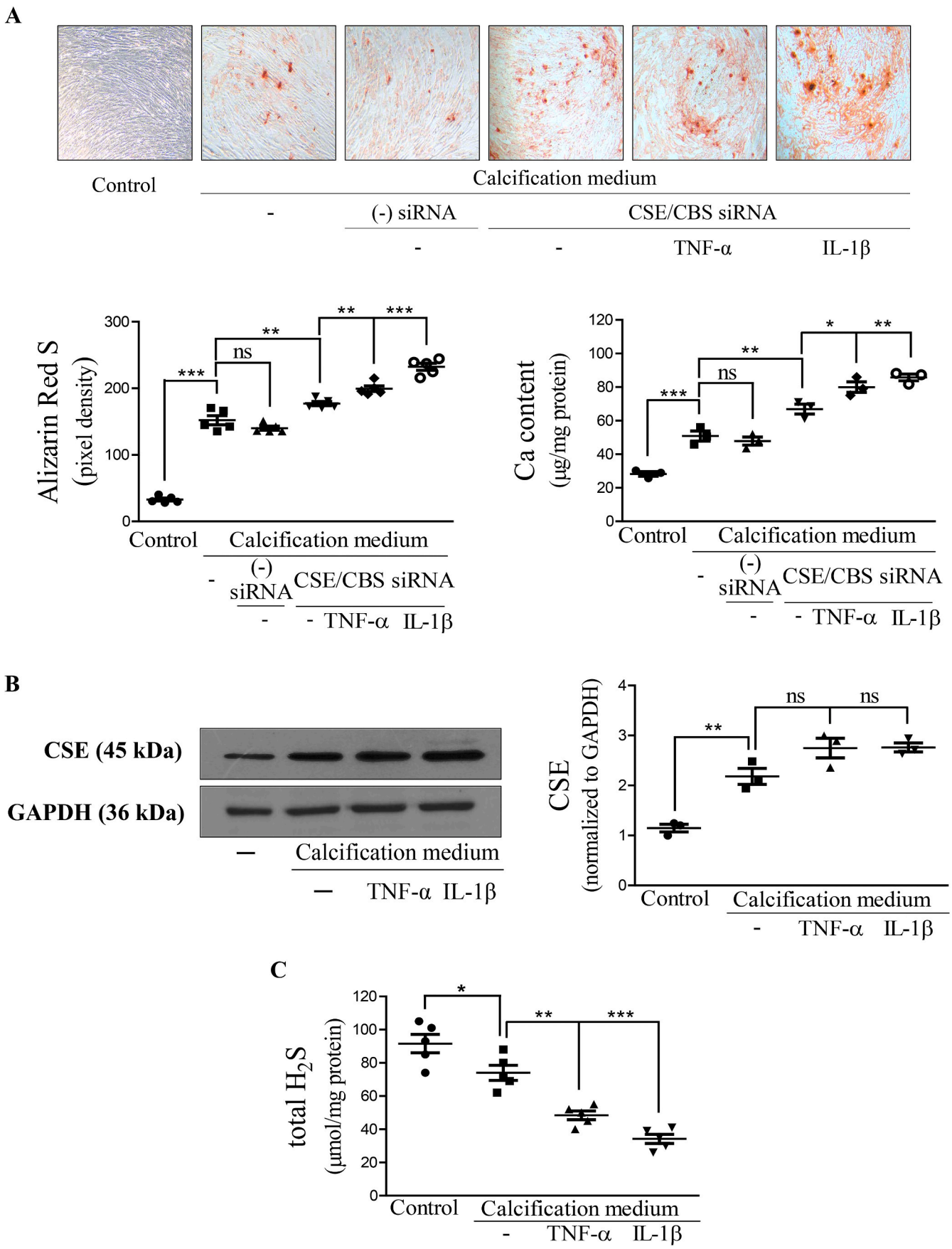

(caption on next page)

Fig. 6. Cystathionine-γ-lyase derived hydrogen sulfide mediates the transient inhibition of calcification in healthy valvular interstitial cells triggered by pro-inflammatory cytokines

CSE and CBS genes were silenced in valvular interstitial cells isolated from healthy aortic valves (HAV-VICs). After the silencing, cells were cultured in a growth medium or exposed to a calcification medium, containing 2.5 mmol/L inorganic phosphate and 1.8 mmol/L calcium chloride every other day, in the presence or absence of TNF-α (10 nmol/L) or IL-1β (10 nmol/L) for 5 days. (A) Alizarin Red S staining of HAV-VICs is shown. Quantitative analysis of Alizarin Red S staining of HAV-VICs was calculated using ImageJ software (n = 5). (A) Calcium contents of extracellular matrix normalized to protein of HAV-VICs are shown (n = 3). (B) CSE protein levels normalized to GAPDH in valvular interstitial cells isolated from calcific aortic valves (CAV-VICs) were measured with western blot (n = 3). Quantitative analysis of the CSE western blots was calculated using ImageJ software (n = 3). (C) H_2S generation measured with modified methylene blue method and normalized to protein of CAV-VICs is shown (n = 5). Results were analyzed by one-way ANOVA, Bonferroni's Multiple Comparison Test, and are shown as mean values ± SEM. Ns: not significant; *$p < 0.05$; **$p < 0.01$; ***$p < 0.001$. (For interpretation of the references to color in this figure legend, the reader is referred to the Web version of this article.)

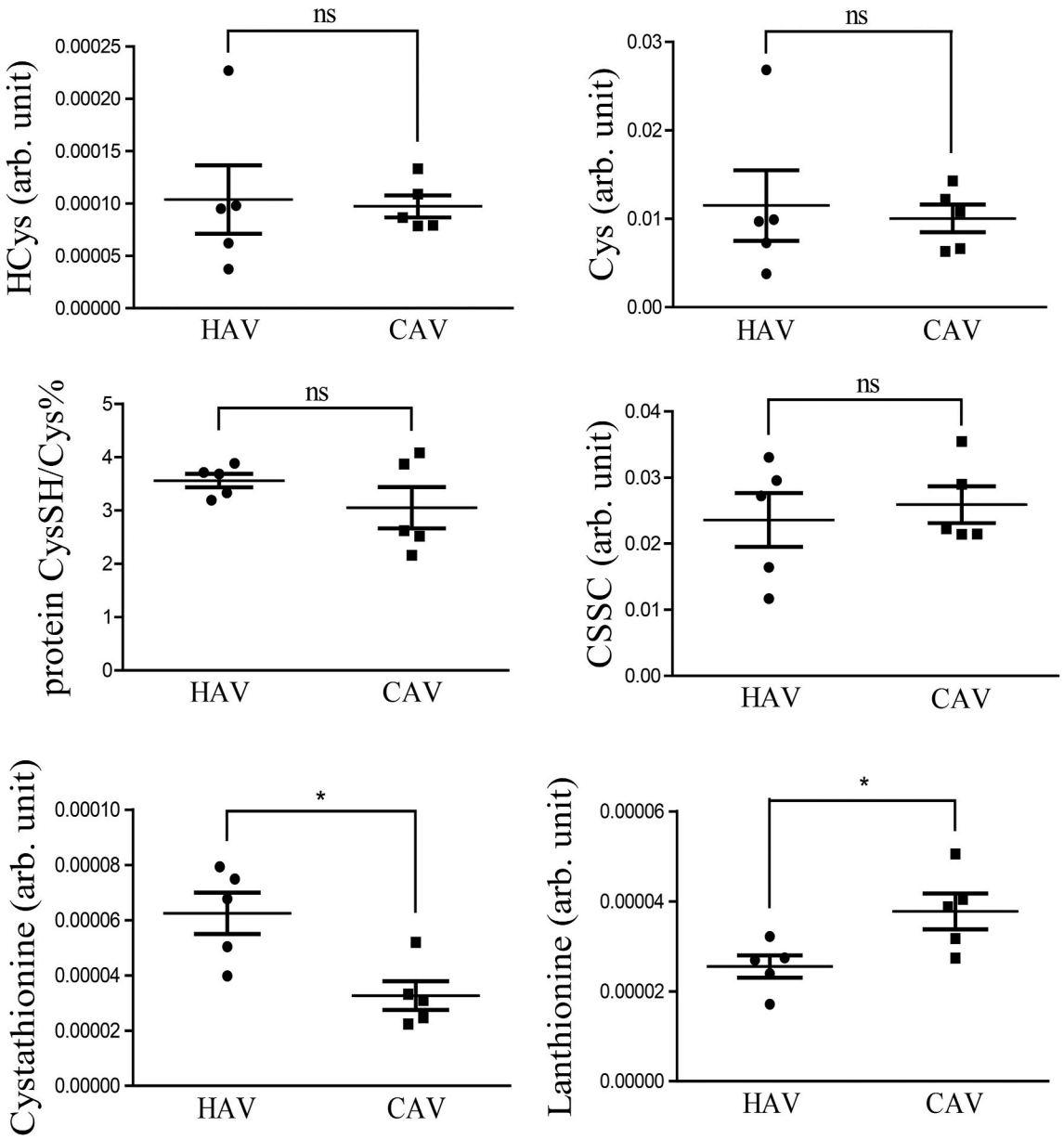

Fig. 7. Cystathionine-γ-lyase is functioning in calcific human aortic valves

Healthy human aortic valves (HAVs) (N = 5) and calcified human aortic valves (CAVs) (N = 5) were cryogenically pulverized and resuspended in CHAPS or RIPA (CysSH/Cys ratios) buffer followed by 10-s sonication on ice. Cys, CSSC, HCys, cystathionine, lanthionine contents and protein CysSH/Cys ratios of the healthy aortic valves (N = 5) and calcified aortic valves (N = 5) are shown. Results were analyzed by unpaired *t*-test, and are shown as mean values ± SEM. Ns: not significant; *$p < 0.05$.

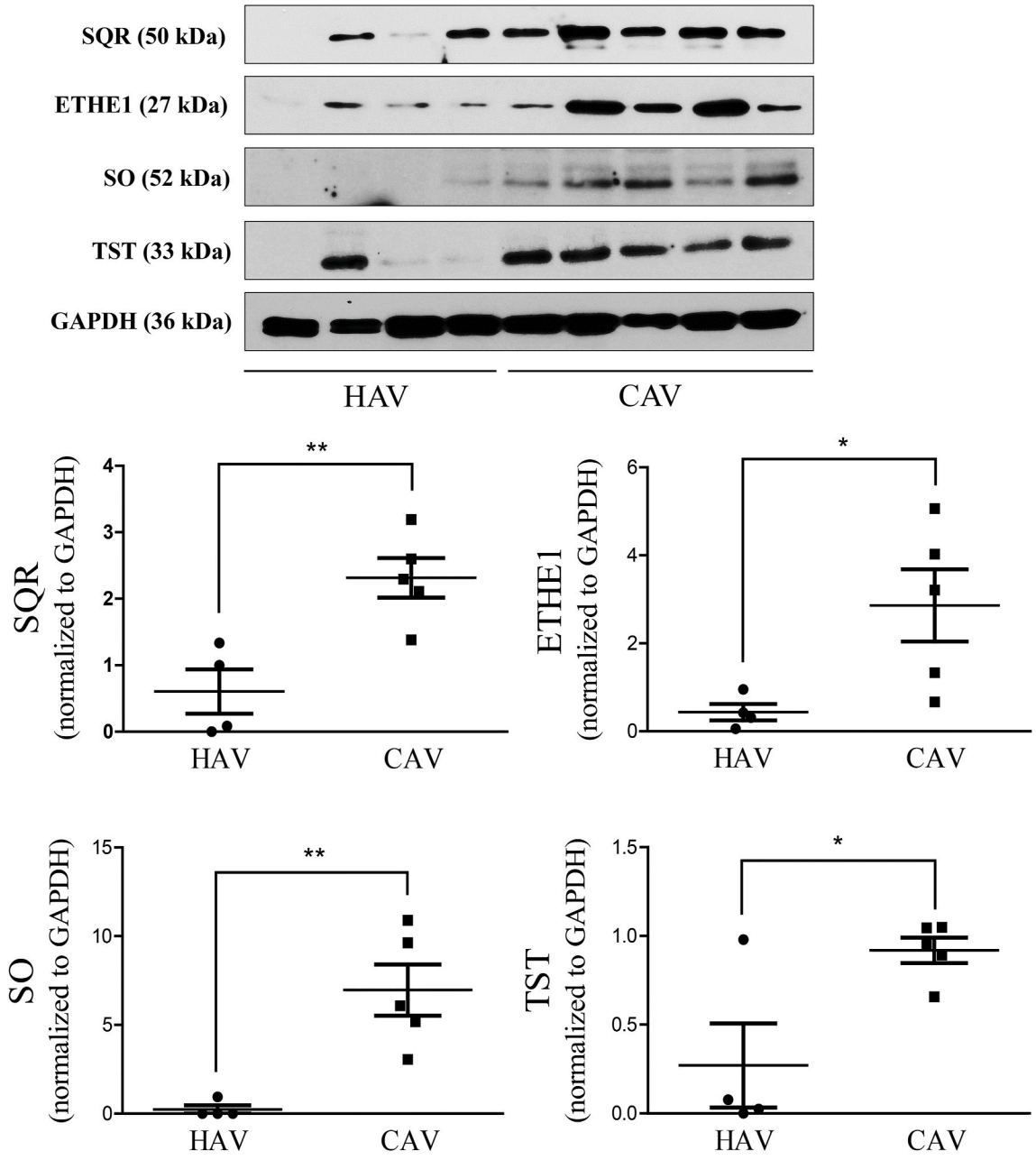

Fig. 8. Mitochondrial enzymes involved in H_2S metabolism are upregulated in calcific human aortic valves
Healthy human aortic valves (HAVs) (N = 4) and calcific human aortic valves (CAVs) (N = 5) were cryogenically pulverized and taken up with cell lysis buffer followed by 5-s sonication on ice three times. SQR, ETHE1, SO and TST protein expression normalized to GAPDH of healthy human aortic valves (N = 4) and calcified human aortic valves (N = 5) were measured with western blot. Quantitative analyses of the SQR, ETHE1, SO and TST western blots were calculated using ImageJ software. Results were analyzed by unpaired *t*-test and were shown as mean values ± SEM. $*p < 0.05$; $**p < 0.01$.

indicative byproduct of H_2S generation by CSE is lanthionine, which is produced when 2 cysteine molecules are used for sulfide synthesis by the enzyme. Hence, we also measured lanthionine levels in aortic valve tissues. Importantly, lanthionine levels were higher in the aortic valve tissues of CAVD patients compared to healthy aortic valves (Fig. 7). These findings together suggest that CSE is fully functional in CAVD and led us to hypothesize that lower levels of observed bioavailable sulfide at increased CSE expressions might be due to an increased metabolic flux of H_2S in the diseased aortic valves. Therefore, we investigated protein levels of SQR, ETHE1, SO and TST, which are enzymes involved in the mitochondrial oxidative catabolism of H_2S. As shown in Fig. 8, the expressions of these enzymes were significantly higher in the calcific aortic valves of CAVD patients compared to healthy aortic valves, which is indeed indicative of an increased sulfide catabolic rate in patient valves and could explain the observed lower steady-state levels of bioavailable sulfide at higher CSE expressions.

These enzymes are also involved in cysteine persulfide metabolism [53,54], therefore taking into account transpersulfidation event we measured the protein persulfidation levels in human healthy and calcified aortic valves. As shown in Fig. 7, there was no difference regarding the protein CysSH/Cys% persulfide levels between healthy and calcified aortic valves.

Since one of the most potent recognized inducers of vascular calcification are elevated plasma phosphate levels [12,13,15], we tested whether phosphate exposure of aortic VICs alters the expression of mitochondrial enzymes involved in H_2S oxidation. Importantly, healthy

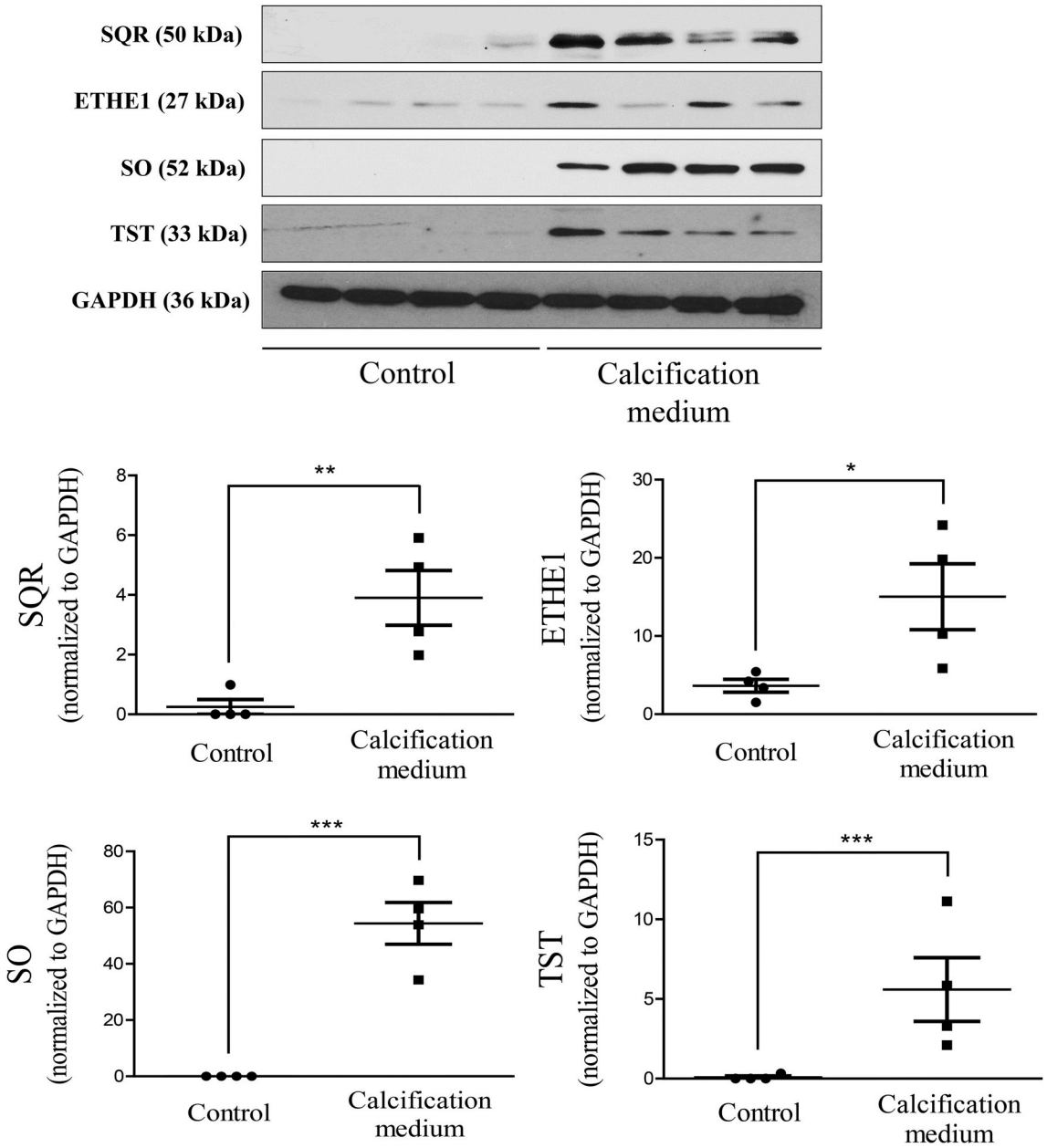

Fig. 9. Valvular interstitial cells of healthy aortic valves exposed to calcifying stimuli up-regulate the expression of SQR, ETHE, SO and TST
Valvular interstitial cells isolated from healthy aortic valves (HAV-VICs) were cultured in a growth medium or exposed to calcification medium, containing 2.5 mmol/L inorganic phosphate and 1.8 mmol/L calcium chloride every other day for 5 days. SQR, ETHE1, SO and TST protein levels normalized to GAPDH were measured with western blot (N = 4). Quantitative analyses of the SQR, ETHE1, SO and TST western blots were calculated using ImageJ software (N = 4). Results were analyzed by unpaired *t*-test and were shown as mean values ± SEM. $*p < 0.05$; $**p < 0.01$; $***p < 0.001$.

VICs cultured at high phosphate levels exhibited increased expression of SQR, and that was accompanied by elevated levels of ETHE1, SO and TST as demonstrated in Fig. 9. This together with the observation that HAV-VICs maintained in high phosphate-containing media for 14 days compared to normal conditions also exhibited elevated expression of CSE and lower H_2S levels (Fig. 5B and C and Fig. 6B and C), suggest that phosphate exposure is indeed an inducer of higher sulfide flux in VICs.

3.7. Mitochondrial sulfide donor prevents calcification provoked by high phosphate levels in human valvular interstitial cells

Mitochondria-targeting H_2S donors [55,56] offer an approach to test if restored H_2S levels in mitochondria could prevent transdifferentiation of VICs to an osteoblastic phenotype in a calcifying environment. We treated cells with compound AP39, a mitochondria-targeting H_2S donor, and measured the calcification of aortic valvular interstitial cells derived from CAVD patients under calcifying conditions. As expected, the transition of VICs to osteoblasts occurred at high phosphate levels as reflected by the accumulation of calcium in the extracellular matrix. Supplementation of H_2S to the mitochondria of VICs by employing AP39 significantly reduced the extracellular calcium deposition as indicated by Alizarin Red staining and direct calcium measurements (Fig. 10A), confirming a key role of mitochondrial H_2S metabolism in maintaining the integrity of the aortic valve.

In order to exclude the effects of cytoplasm H_2S in our experiments we employed NaSH (general H_2S donor) and compared its impact with AP39. As shown in Supplementary Fig. 1, the optimal concentration of AP39 in the inhibition of VICs calcification provoked by high phosphate

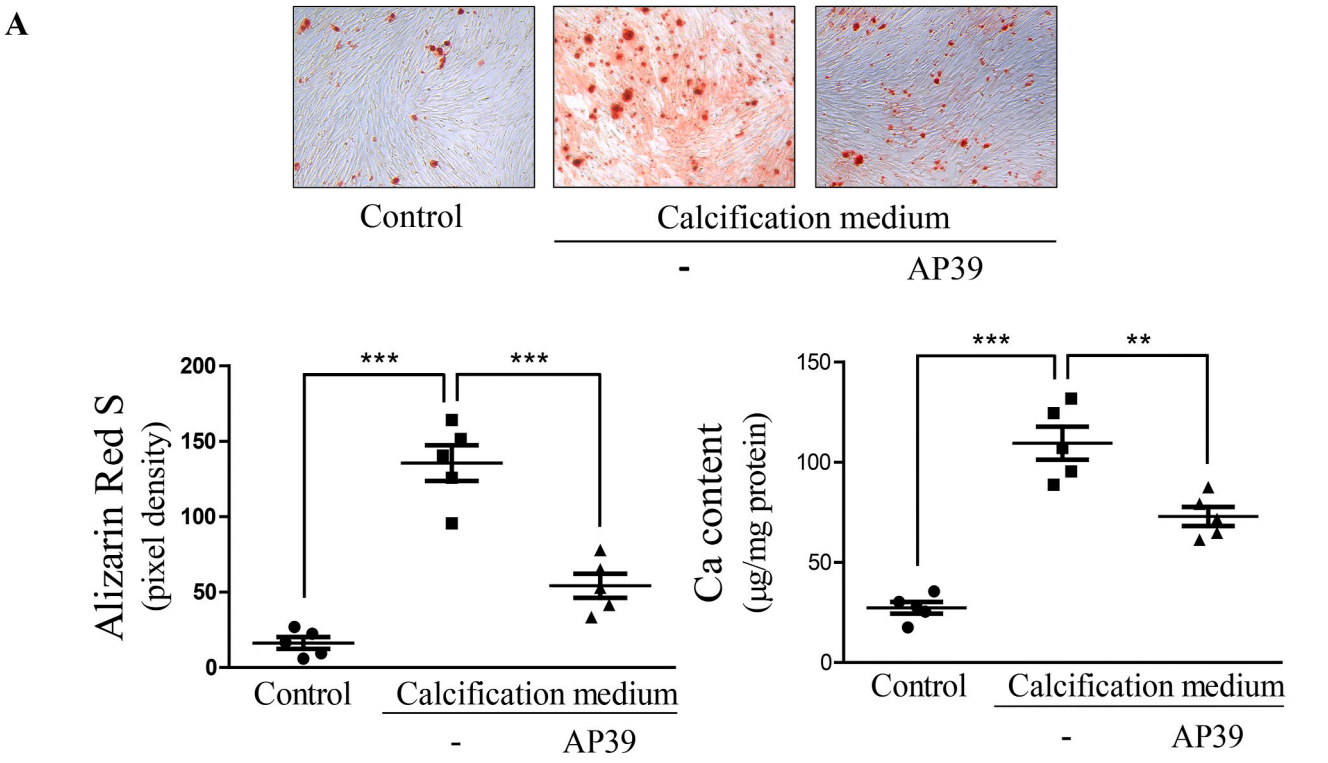

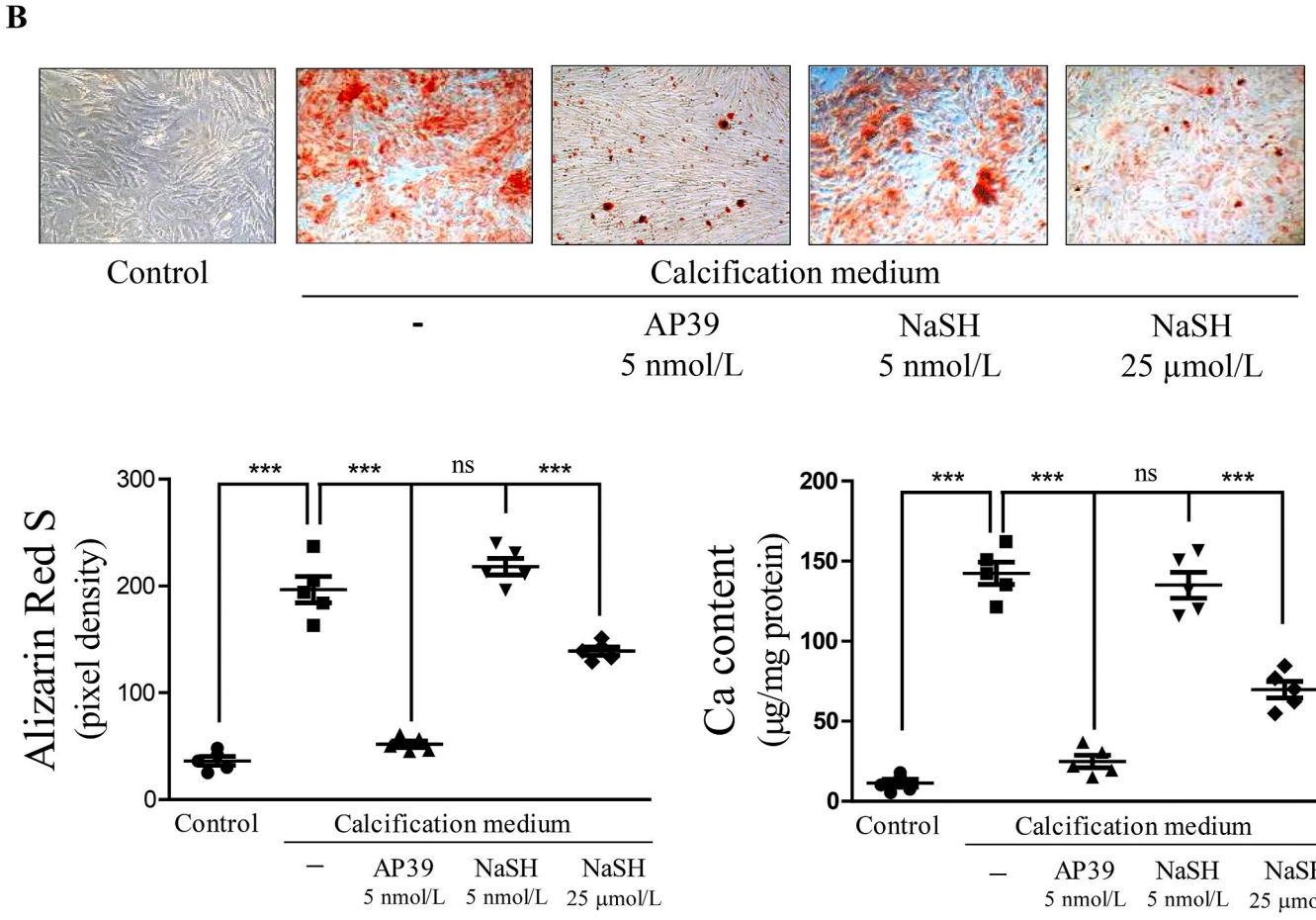

(caption on next page)

Fig. 10. Mitochondria-targeting H_2S donor prevents calcification of valvular interstitial cells derived from calcific human aortic valves
Valvular interstitial cells isolated from calcific aortic valves (CAV-VICs) were cultured in a growth medium or exposed to calcification medium containing 2.5 mmol/L inorganic phosphate and 1.8 mmol/L calcium chloride every other day in the presence or absence of [10-oxo-10-[4-(3-thioxo-3H-1,2-dithiol-5-yl)phenoxy]decyl] triphenyl-phosphonium (AP39) (5 nmol/L) or sodium hydrogen sulfide (NaSH) (5 nmol/L; 25 μmol/L) for 5 days. (A and B) Alizarin Red S staining and extracellular calcium content normalized to protein of CAV-VICs are shown (n = 5). Quantitative analysis of Alizarin Red S staining of CAV-VICs was performed using ImageJ software (n = 5). Results were analyzed by one-way ANOVA, Bonferroni's Multiple Comparison Test, and were shown as mean values ± SEM. Ns: not significant; $^{**}p < 0.01$; $^{***}p < 0.001$. (For interpretation of the references to color in this figure legend, the reader is referred to the Web version of this article.)

was 5 nmol/L. In contrast, NaSH failed to affect the calcification of VICs at concentration of 5 nmol/L (Supplementary Fig. 1). Similar suppression on VICs calcification provided by 5 nmol/L AP39 was found to occur when 25 μmol/L of NaSH was used (Fig. 10 and Supplementary Fig. 2). When we compared the effectiveness of AP39 and NaSH in the inhibition of VICs calcification, AP39 was more effective by 59.8 ± 8% at 5000 times lower concentration (Fig. 10).

3.8. Mitochondrial sulfide donor prevents inflammation provoked by high phosphate levels in human valvular interstitial cells

Since calcification and inflammation are connected in the pathogenesis of CAVD [1,5,6,43] we tested whether AP39 also affects inflammation of VICs. As expected, the expression of inflammatory cytokines, IL-1β and TNF-α were increased in human interstitial cells maintained in calcifying media at both mRNA and protein levels (Fig. 11A–C). Treatment of cells with AP39 resulted in the loss of elevation of pro-inflammatory cytokines provoked by high phosphate levels (Fig. 11A–C). We also performed immunofluorescence staining using STED-CW nanoscopy for calcification, formation of hydroxyapatite (Osteosense) as well as IL-1β and TNF-α in VICs maintained in calcifying milieu with or without AP39 treatment. As shown in Fig. 11C, accumulation of calcium in the extracellular matrix occurred when cells were cultured in high phosphate media and that was accompanied by strong staining for IL-1β and TNF-α in VICs. Importantly, AP39 treatment significantly inhibited the accumulation of calcium in extracellular matrix and prevented the expression of IL-1β and TNF-α (Fig. 11C).

4. Discussion

This study is the first that highlights the relationship between the metabolic control of H_2S levels in human aortic VICs and the calcification process in the aortic valves of CAVD patients. Lower levels of H_2S were detected, which was accompanied by higher expression of the H_2S generating enzyme CSE (Fig. 1C) as well as by higher expression of mitochondrial enzymes involved in H_2S oxidation in the aortic valves of CAVD patients compared to healthy aortic valves (Fig. 8). In accordance, healthy human aortic VICs under calcifying conditions mimic the transsulfuration enzyme expression profile of this human pathology, because elevated CSE expression (Fig. 5B) was associated with elevated expressions of SQR, the key enzyme in mitochondrial H_2S oxidation as well as its downstream enzymes ETHE1, SO and TST (Fig. 9). We propose that the lower observed bioavailable H_2S levels (Fig. 5C) in VICs under these conditions as well as in CAVD aortic valves is due to a calcifying environment-induced increased mitochondrial consumption rate of sulfide.

Although the increased catabolism of H_2S could explain the observed lower bioavailable H_2S levels, some caveats of this notion are acknowledged. The high CSE expression may not necessarily be associated with high H_2S production rates in these valvular lesions. Alternatively, CSE phosphorylation at Ser377 could lead to decreased activity of the enzyme [57]. Nevertheless, the increased lanthionine levels observed in aortic valves of CAVD patients compared to healthy tissues suggested that CSE is fully active and H_2S generation rates may even be elevated in CAVD (Fig. 7).

Altered expression of CBS would offer another explanation for the low bioavailable H_2S levels in CAVD. Immunohistochemistry and western blot analyses revealed that expression of CBS in calcific aortic valves is similar to that observed in healthy aortic valve (Fig. 2). This suggests that the lower bioavailable H_2S levels observed in CAVD are not related to CBS.

H_2S is an important signaling molecule that has gained increasing attention in recent years due to its versatile functions in cardiovascular systems [18,20,21]. Our laboratory has previously shown that endogenous production of H_2S by CSE and H_2S administration via sulfide releasing molecules inhibit aortic valve calcification in $ApoE^{-/-}$ mouse as well as the transdifferentiation of human VICs and human vascular smooth muscle cells towards osteoblast-like cells [27,42].

Due to the suggested interactions of Cys-persulfide with the mitochondrial electron transport chain, enzymes activating during H_2S catabolism, including SQR, ETHE1, SO, and TST may also be enhanced during persulfide/polysulfide metabolism [53,54]. In addition, generation of H_2S can also be an indicative event for increased levels of persulfide/polysulfide or their metabolism [58–63]. It should also be noted that the currently available state-of-the-art detection protocols to measure reactive sulfur species (including H_2S) can artificially alter their speciation [60,61]. Therefore, at present it is very difficult to distinguish whether the observed biological effect is mediated by H_2S or persulfides/polysulfides. Nevertheless, we measured total protein persulfidation levels in human healthy and calcified aortic valves. We observed unaltered protein CysSH/Cys% persulfide levels, which for the above mentioned detection problems (discussed in detail in the cited references) do not explicitely exclude the role of persulfides nor support the direct role of H_2S in our study systems (Fig. 7).

It has been revealed that increased expression of pro-inflammatory cytokines, IL-1β and TNF-α are associated with CAVD, and inflammation is a hallmark of CAVD [1–3,5]. CAVD was shown to be an active complex osteogenic process and inflammation plays a central role in its initiation and progression. These observations prompted us to study the effects of IL-1β and TNF-α on human VICs under calcifying conditions. As previously revealed, both IL-1β and TNF-α facilitated calcification of human VICs regardless of cellular origin, more specifically whether they are derived from aortic valves of healthy individuals or CAVD patients (Fig. 3). Although there are robust differences regarding the extent and time course of cellular responses depending upon the cellular origin as reflected by calcification and production of inflammatory cytokines, the ultimate directions of these responses were the same (Fig. 3). The calcification was more rapid and the synthesis of IL-1β and TNF-α were more pronounced in cells of CAVD patients (Fig. 3), which might be due to their inherited osteoblastic commitment derived from the calcifying milieu in the diseased valves.

As shown by Lagoutte and colleagues [34], H_2S has a substantial role in mammalian cell bioenergetics via stimulating the mitochondrial electron transport chain. Studies with the mitochondria-targeting H_2S donor, AP39, have been shown to exert beneficial effects on bioenergetic parameters [55,56]. Therefore, we tested whether restoration of H_2S levels in mitochondria via a mitochondria-targeting H_2S donor might represent an approach to control the calcification of VICs. The anti-calcification action of AP39 observed on human aortic VICs supports the essential role of mitochondrial H_2S metabolism in maintaining the integrity of the aortic valve (Figs. 10 and 11).

H_2S measurements in our studies were not specific for the mitochondria, therefore we performed experiments using NaSH (general H_2S donor) and compared it with AP39 to rule out the effects of cytoplasmic H_2S in the observed inhibition of VICs calcification. NaSH failed to affect calcification of VICs at 5 nmol/L, an optimal concentration for AP39

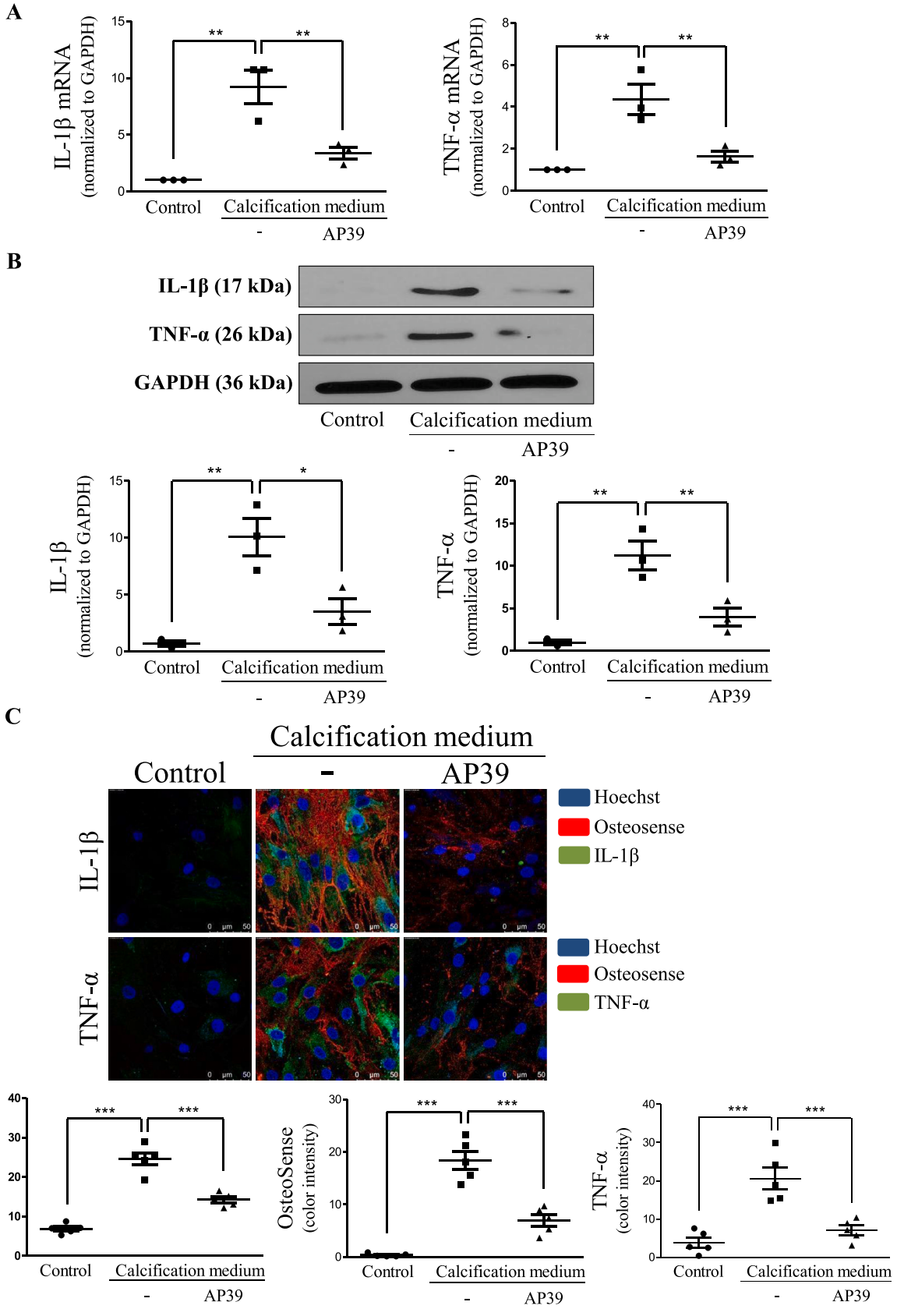

(caption on next page)

Fig. 11. Mitochondria-targeting H_2S donor inhibits inflammation of valvular interstitial cells
Valvular interstitial cells (VICs) isolated from healthy aortic valves (HAV-VICs) were cultured in growth medium or calcification medium, containing 2.5 mmol/L inorganic phosphate and 1.8 mmol/L calcium chloride every other day, in the presence or absence of [10-oxo-10-[4-(3-thioxo-3H-1,2-dithiol-5-yl)phenoxy]decyl] triphenyl-phosphonium (AP39) (5 nmol/L) for 5 days. (A) Relative expression of IL-1β (left panel) and TNF-α (right panel) were analyzed by Real-Time qPCR (n = 3) in HAV-VICs are shown. (B) Protein expression of IL-1β, TNF-α, and GAPDH were determined by western blots in HAV-VICs are shown. Quantification of IL-1β and TNF-α optical density was calculated by ImageJ software. (C) HAV-VICs grown on coverslips and cultured in growth medium or calcification medium, containing 2.5 mmol/L inorganic phosphate and 1.8 mmol/L calcium chloride every other day, in the presence or absence of AP39 (5 nmol/L) for 5 days. Cells were stained with Hoechst 33258 for DNA (blue), an anti-IL-1β antibody with Alexa Fluor 488 secondary antibody for IL-1β (green), an anti-TNF-α antibody with Alexa Fluor 488 secondary antibody for TNF-α (green), and with Osteosense Fluorescent Probe (red). Images were taken with Leica TCS SP8 gated STED-CW nanoscopy. Images were deconvolved using Huygens Professional software. The color intensity of IL-1β, TNF-α, and Osteosense stainings was calculated using ImageJ software. Representative image, n = 5. Scale bars shown in the images represent 50 μm. Results were analyzed by one-way ANOVA, Bonferroni's Multiple Comparison Test, and were shown as mean values ± SEM. *$p < 0.05$; **$p < 0.01$; ***$p < 0.001$. (For interpretation of the references to color in this figure legend, the reader is referred to the Web version of this article.)

(Fig. 10 and Suppl. Fig. 1). When we compared the effectiveness of AP39 and NaSH, the mitochondria-targeting H_2S donor AP39 was more effective at 5000 times lower concentration indicating that mitochondrial H_2S plays a critical role in the inhibition of calcification of VICs (Fig. 10 and Suppl. Fig. 1). Retardation of calcification and the decreased expression of pro-inflammatory cytokines resulted from AP39 treatment at such a low concentrations are in accordance with previous observation revealing the pathophysiological connection between calcification and inflammation in CAVD [1,5,6,43] (Fig. 11).

Importantly and to our surprise, we observed a transient inhibition of VICs calcification and osteoblastic phenotype switch in response to IL-1β and TNF-α in cells derived from the healthy aortic valves, as opposed to cells of CAVD patients (Fig. 4A–D). This benefit might also be linked to H_2S biogenesis, as both IL-1β and TNF-α enhanced the expression of CSE along with an observed increase in H_2S levels (Fig. 5B and C). To test whether CSE-derived H_2S is responsible for the inhibition of calcification and osteoblastic transition of VICs we silenced the expression of CSE and CBS. A number of studies in different biological systems revealed that, considering sulfide/persulfide producing activities, CSE and CBS can to some extent compensate for each other [29,64,65], thus we employed double silencing of these enzymes. The reduction of endogenous H_2S production led to the loss of anti-calcification effects under calcifying conditions indicating that CSE-derived H_2S might be responsible for the transient inhibition of human VICs calcification, which was induced by TNF-α or IL-1β (Fig. 6).

Similarly to VICs, CSE expression can be enhanced by TNF-α and IL-1β in other cells in the vasculature including smooth muscle cells, endothelium and macrophages. CSE is also inducible by other substances involved in vascular pathologies such as peroxides associated with oxLDL and atherosclerotic plaque lipids, as well as heme or oxidized hemoglobin [52]. These constituents were also strongly associated with the development of CAVD [1,5] and could contribute to the elevated expression of CSE in aortic valves.

5. Conclusions

We propose that in a calcifying milieu [1,5] depletion of H_2S by enhanced mitochondrial catabolic rates may facilitate VICs calcification in CAVD, and up-regulation of CSE represents an adaptive anti-calcification rescue mechanism via generation of protecting H_2S.

Author contributions

Conception or design of the work: JB, PN, ZSC, LP, KÉS. Data collection: ZSC, LP, KÉS, TD, EPJ, KG, LB, DY, RT. Data analysis and interpretation: ZSC, LP, KÉS, GM, GyB, PN, JB. Drafting the article: JB, LP, ZSC, PN, GyB, TD, EPJ, KG. Critical revision of the article: JB, PN, MW, GyB. Final approval of the version to be published: JB, PN, GyB. Specimen collection: TSZ, ZH, PG, LB.

Declaration of competing interest

All the authors declared no competing interests. MW has patent applications for the therapeutic use of slow hydrogen sulfide donor molecules.

Data availability

No data was used for the research described in the article.

Acknowledgments

The research group is supported by Eötvös Loránd Research Network (11003). This work was supported by Hungarian Government grants, OTKA-K 132828 (J.B.). The project was co-financed by the European Union and the European Social Fund: GINOP-2.3.2-15-2016-00043 (IRONHEARTH) and EFOP-3.6.2-16-2017-00006 (LIVE LONGER). Project no. TKP2020-NKA-04 has been implemented with the support provided by the Ministry of Innovation and Technology of Hungary from the National Research, Development and Innovation Fund, financed under the 2020-4.1.1-TKP2020 funding scheme. Project no. TKP2021-EGA-18 has been implemented with the support provided by the Ministry of Innovation and Technology of Hungary from the National Research, Development and Innovation Fund, financed under the TKP2021-EGA funding scheme. P.N. acknowledges financial support from the National Laboratories Program (under the National Tumor Biology Laboratory (2022-2.1.1-NL-2022-00010)), the Hungarian Thematic Excellence Program (under project TKP2021-EGA-44) from the Hungarian National Research, Development and Innovation Office as well as Eötvös Loránd Research Network – ATE- Laboratory of Redox Biology (grant 15002) from the Hungarian Academy of Sciences. K.G acknowledges financial support from the Richter Gedeon Talentum Foundation founded by Richter Gedeon Plc. The work was carried out at the University of Debrecen, Kálmán Laki Doctoral School of Biomedical and Clinical Sciences. Authors thank Ibolya Fürtös for her excellent technical assistance.

Appendix A. Supplementary data

Supplementary data to this article can be found online at https://doi.org/10.1016/j.redox.2023.102629.

References

[1] K.E. Yutzey, et al., Calcific aortic valve disease: a consensus summary from the alliance of investigators on calcific aortic valve disease, Arterioscler. Thromb. Vasc. Biol. 34 (11) (2014) 2387–2393.
[2] K.D. O'Brien, et al., Osteopontin is expressed in human aortic valvular lesions, Circulation 92 (8) (1995) 2163–2168.
[3] E.R. Mohler 3rd, et al., Bone formation and inflammation in cardiac valves, Circulation 103 (11) (2001) 1522–1528.
[4] R.V. Freeman, C.M. Otto, Spectrum of calcific aortic valve disease: pathogenesis, disease progression, and treatment strategies, Circulation 111 (24) (2005) 3316–3326.

[5] N.M. Rajamannan, et al., Calcific aortic valve disease: not simply a degenerative process: a review and agenda for research from the National Heart and Lung and Blood Institute Aortic Stenosis Working Group. Executive summary: calcific aortic valve disease-2011 update, Circulation 124 (16) (2011) 1783–1791.
[6] N. Coté, et al., Inflammation is associated with the remodeling of calcific aortic valve disease, Inflammation 36 (3) (2013) 573–581.
[7] N.M. Rajamannan, et al., Human aortic valve calcification is associated with an osteoblast phenotype, Circulation 107 (17) (2003) 2181–2184.
[8] C.M. Giachelli, The emerging role of phosphate in vascular calcification, Kidney Int. 75 (9) (2009) 890–897.
[9] P. Raggi, et al., Cardiac calcification in adult hemodialysis patients. A link between end-stage renal disease and cardiovascular disease? J. Am. Coll. Cardiol. 39 (4) (2002) 695–701.
[10] G.A. Block, et al., Association of serum phosphorus and calcium x phosphate product with mortality risk in chronic hemodialysis patients: a national study, Am. J. Kidney Dis. 31 (4) (1998) 607–617.
[11] B. Kestenbaum, et al., Serum phosphate levels and mortality risk among people with chronic kidney disease, J. Am. Soc. Nephrol. 16 (2) (2005) 520–528.
[12] W.G. Goodman, et al., Coronary-artery calcification in young adults with end-stage renal disease who are undergoing dialysis, N. Engl. J. Med. 342 (20) (2000) 1478–1483.
[13] G.M. London, et al., Arterial media calcification in end-stage renal disease: impact on all-cause and cardiovascular mortality, Nephrol. Dial. Transplant. 18 (9) (2003) 1731–1740.
[14] K.A. Hruska, et al., Hyperphosphatemia of chronic kidney disease, Kidney Int. 74 (2) (2008) 148–157.
[15] S. Jono, et al., Phosphate regulation of vascular smooth muscle cell calcification, Circ. Res. 87 (7) (2000) E10–E17.
[16] C.M. Giachelli, et al., Vascular calcification and inorganic phosphate, Am. J. Kidney Dis. 38 (4 Suppl 1) (2001) S34–S37.
[17] S.A. Steitz, et al., Smooth muscle cell phenotypic transition associated with calcification: upregulation of Cbfa1 and downregulation of smooth muscle lineage markers, Circ. Res. 89 (12) (2001) 1147–1154.
[18] S.C. Bir, C.G. Kevil, Sulfane sustains vascular health: insights into cystathionine γ-lyase function, Circulation 127 (25) (2013) 2472–2474.
[19] N.L. Kanagy, C. Szabo, A. Papapetropoulos, Vascular biology of hydrogen sulfide, Am. J. Physiol. Cell Physiol. 312 (5) (2017) C537–c549.
[20] K.R. Olson, N.L. Whitfield, Hydrogen sulfide and oxygen sensing in the cardiovascular system, Antioxidants Redox Signal. 12 (10) (2010) 1219–1234.
[21] N. Dilek, et al., Hydrogen sulfide: an endogenous regulator of the immune system, Pharmacol. Res. 161 (2020), 105119.
[22] M. Li, J. Mao, Y. Zhu, New therapeutic approaches using hydrogen sulfide donors in inflammation and immune response, Antioxidants Redox Signal. 35 (5) (2021) 341–356.
[23] A. Ahmad, et al., AP39, A mitochondrially targeted hydrogen sulfide donor, exerts protective effects in renal epithelial cells subjected to oxidative stress in vitro and in acute renal injury in vivo, Shock 45 (1) (2016) 88–97.
[24] S. Mani, et al., Decreased endogenous production of hydrogen sulfide accelerates atherosclerosis, Circulation 127 (25) (2013) 2523–2534.
[25] S. Yuan, et al., Cystathionine γ-lyase modulates flow-dependent vascular remodeling, Arterioscler. Thromb. Vasc. Biol. 38 (9) (2018) 2126–2136.
[26] H.L. Jiang, et al., [Changes of the new gaseous transmitter H2S in patients with coronary heart disease], Di Yi Jun Yi Da Xue Xue Bao 25 (8) (2005) 951–954.
[27] E. Zavaczki, et al., Hydrogen sulfide inhibits the calcification and osteoblastic differentiation of vascular smooth muscle cells, Kidney Int. 80 (7) (2011) 731–739.
[28] A. Longchamp, et al., Plasma hydrogen sulfide is positively associated with post-operative survival in patients undergoing surgical revascularization, Front Cardiovasc Med 8 (2021), 750926.
[29] V. Kožich, et al., Human ultrarare genetic disorders of sulfur metabolism demonstrate redundancies in H2S homeostasis, Redox Biol. (2022), 102517.
[30] O. Kabil, et al., The quantitative significance of the transsulfuration enzymes for H2S production in murine tissues, Antioxidants Redox Signal. 15 (2) (2011) 363–372.
[31] X. Chen, K.H. Jhee, W.D. Kruger, Production of the neuromodulator H2S by cystathionine beta-synthase via the condensation of cysteine and homocysteine, J. Biol. Chem. 279 (50) (2004) 52082–52086.
[32] D.L. Nandi, P.M. Horowitz, J. Westley, Rhodanese as a thioredoxin oxidase, Int. J. Biochem. Cell Biol. 32 (4) (2000) 465–473.
[33] T.M. Hildebrandt, M.K. Grieshaber, Three enzymatic activities catalyze the oxidation of sulfide to thiosulfate in mammalian and invertebrate mitochondria, FEBS J. 275 (13) (2008) 3352–3361.
[34] E. Lagoutte, et al., Oxidation of hydrogen sulfide remains a priority in mammalian cells and causes reverse electron transfer in colonocytes, Biochim. Biophys. Acta 1797 (8) (2010) 1500–1511.
[35] M.R. Jackson, S.L. Melideo, M.S. Jorns, Human sulfide:quinone oxidoreductase catalyzes the first step in hydrogen sulfide metabolism and produces a sulfane sulfur metabolite, Biochemistry 51 (34) (2012) 6804–6815.
[36] O. Kabil, R. Banerjee, Characterization of patient mutations in human persulfide dioxygenase (ETHE1) involved in H2S catabolism, J. Biol. Chem. 287 (53) (2012) 44561–44567.
[37] M. Libiad, A. Sriraman, R. Banerjee, Polymorphic variants of human rhodanese exhibit differences in thermal stability and sulfur transfer kinetics, J. Biol. Chem. 290 (39) (2015) 23579–23588.
[38] U. Kappler, J.H. Enemark, Sulfite-oxidizing enzymes, J. Biol. Inorg. Chem. 20 (2) (2015) 253–264.
[39] A.T. Mellis, et al., The role of glutamate oxaloacetate transaminases in sulfite biosynthesis and H(2)S metabolism, Redox Biol. 38 (2021), 101800.
[40] S. Le Trionnaire, et al., The synthesis and functional evaluation of a mitochondria-targeted hydrogen sulfide donor, (10-oxo-10-(4-(3-thioxo-3H-1,2-dithiol-5-yl) phenoxy)decyl)triphenylphosphonium bromide (AP39), MedChemComm 5 (6) (2014) 728–736.
[41] Q.G. Karwi, et al., AP39, a mitochondria-targeting hydrogen sulfide (H(2) S) donor, protects against myocardial reperfusion injury independently of salvage kinase signalling, Br. J. Pharmacol. 174 (4) (2017) 287–301.
[42] K. Sikura, et al., Hydrogen sulfide inhibits calcification of heart valves; implications for calcific aortic valve disease, Br. J. Pharmacol. 177 (4) (2020) 793–809.
[43] K. Éva Sikura, et al., Hydrogen sulfide inhibits aortic valve calcification in heart via regulating RUNX2 by NF-κB, a link between inflammation and mineralization, J. Adv. Res. 27 (2021) 165–176.
[44] M. Kulkarni-Chitnis, et al., Inhibitory action of novel hydrogen sulfide donors on bovine isolated posterior ciliary arteries, Exp. Eye Res. 134 (2015) 73–79.
[45] L. Li, et al., Characterization of a novel, water-soluble hydrogen sulfide-releasing molecule (GYY4137): new insights into the biology of hydrogen sulfide, Circulation 117 (18) (2008) 2351–2360.
[46] M. Whiteman, et al., Phosphinodithioate and phosphoramidodithioate hydrogen sulfide donors, Handb. Exp. Pharmacol. 230 (2015) 337–363.
[47] R.A. Gould, J.T. Butcher, Isolation of valvular endothelial cells, JoVE (46) (2010).
[48] N. Gilboa-Garber, Direct spectrophotometric determination of inorganic sulfide in biological materials and in other complex mixtures, Anal. Biochem. 43 (1) (1971) 129–133.
[49] A.D. Ang, et al., Measuring free tissue sulfide, Adv. Biol. Chem. (2012) 6. Vol.02No.04.
[50] V. Kožich, et al., Thioethers as markers of hydrogen sulfide production in homocystinurias, Biochimie 126 (2016) 14–20.
[51] T. Akaike, et al., Cysteinyl-tRNA synthetase governs cysteine polysulfidation and mitochondrial bioenergetics 8 (1) (2017) 1177.
[52] L. Potor, et al., Hydrogen Sulfide Abrogates Hemoglobin-Lipid Interaction in Atherosclerotic Lesion 2018, 2018, 3812568.
[53] E. Marutani, et al., Sulfide catabolism ameliorates hypoxic brain injury, Nat. Commun. 12 (1) (2021) 3108.
[54] T. Akaike, et al., Cysteinyl-tRNA synthetase governs cysteine polysulfidation and mitochondrial bioenergetics, Nat. Commun. 8 (1) (2017) 1177.
[55] B. Szczesny, et al., AP39, a novel mitochondria-targeted hydrogen sulfide donor, stimulates cellular bioenergetics, exerts cytoprotective effects and protects against the loss of mitochondrial DNA integrity in oxidatively stressed endothelial cells in vitro, Nitric Oxide 41 (2014) 120–130.
[56] D. Gerő, et al., The novel mitochondria-targeted hydrogen sulfide (H(2)S) donors AP123 and AP39 protect against hyperglycemic injury in microvascular endothelial cells in vitro, Pharmacol. Res. 113 (Pt A) (2016) 186–198.
[57] S.I. Bibli, et al., Cystathionine γ lyase sulfhydrates the RNA binding protein human antigen R to preserve endothelial cell function and delay atherogenesis, Circulation 139 (1) (2019) 101–114.
[58] É. Dóka, et al., A novel persulfide detection method reveals protein persulfide- and polysulfide-reducing functions of thioredoxin and glutathione systems, Sci. Adv. 2 (1) (2016) e1500968.
[59] R. Wedmann, et al., Improved tag-switch method reveals that thioredoxin acts as depersulfidase and controls the intracellular levels of protein persulfidation, Chem. Sci. 7 (5) (2016) 3414–3426.
[60] V. Bogdándi, et al., Speciation of reactive sulfur species and their reactions with alkylating agents: do we have any clue about what is present inside the cell? Br. J. Pharmacol. 176 (4) (2019) 646–670.
[61] P. Nagy, et al., Measuring reactive sulfur species and thiol oxidation states: challenges and cautions in relation to alkylation-based protocols, Antioxidants Redox Signal. 33 (16) (2020) 1174–1189.
[62] T. Ditrói, et al., Comprehensive analysis of how experimental parameters affect H (2)S measurements by the monobromobimane method, Free Radic. Biol. Med. 136 (2019) 146–158.
[63] X. Shen, et al., Analytical measurement of discrete hydrogen sulfide pools in biological specimens, Free Radic. Biol. Med. 52 (11–12) (2012) 2276–2283.
[64] S.S. Nandi, P.K. Mishra, H(2)S and homocysteine control a novel feedback regulation of cystathionine beta synthase and cystathionine gamma lyase in cardiomyocytes, Sci. Rep. 7 (1) (2017) 3639.
[65] K. Erdélyi, et al., Reprogrammed Transsulfuration Promotes Basal-like Breast Tumor Progression via Realigning Cellular Cysteine Persulfidation, 118, 2021, 45.